2022, Instituto Mexicano de Tecnología del Agua

Open Access bajo la licencia CC BY-NC-SA 4.0
(https://creativecommons.org/licenses/by-nc-sa/4.0/)

DOI: 10.24850/j-tyca-2022-01-09

Articles

Determination of design parameters of submerged breakwater by means of numeric simulation for their employment in beaches

Determinación de parámetros de diseño de rompeolas sumergidos mediante simulación numérica para su empleo en playas

Kenia Hernández-Valdés[1], ORCID: https://orcid.org/0000-0003-0373-2592

Luis Fermín Córdova-López[2], ORCID: https://orcid.org/ 0000-0001-8175-6819

[1]Inversiones Gamma S.A, La Habana, Cuba, kenia@gamma.com.cu

[2]Universidad Tecnológica de La Habana, Cuba, cordova@tesla.cujae.edu.cu

Corresponding author: Kenia Hernández-Valdés, kenia@gamma.com.cu

Abstract

2022, Instituto Mexicano de Tecnología del Agua

Open Access bajo la licencia CC BY-NC-SA 4.0
(https://creativecommons.org/licenses/by-nc-sa/4.0/)

The necessity to implement solutions that guarantee the protection and recovery of the coastal area makes that the submerged breakwater employment is evaluated as a viable variant of application because these works contribute to the conservation of the natural and aesthetic conditions of the beaches, which is part of the tourist product that is marketed. However, the parameters that intervene in their functional design are not very well established, propitiating in many cases circulation patterns in the currents that contribute to the erosion and the degradation of the coast. The present work is part of the development of the Coastal and Marine Engineering System (SICOM) that carries out the Hydraulic Investigations Center of the Technological University of Havana, centered in to simulate so much the hydrodynamic changes as morphological that happen in the Cuban beaches before the presence of submerged breakwater, and in obtaining the design parameters for the employment of these works in the mitigation of the erosion of the beaches, using numeric models as predictive tools.

Keywords: Submerged breakwater, morphological changes, numeric models.

Resumen

La necesidad de implementar soluciones que garanticen la protección y recuperación de la zona costera hace que se evalúe el empleo de rompeolas sumergidos como una variante viable de aplicación, pues estas obras contribuyen a la conservación de las condiciones naturales, estéticas y paisajísticas de las playas, lo que forma parte del producto

2022, Instituto Mexicano de Tecnología del Agua

Open Access bajo la licencia CC BY-NC-SA 4.0
(https://creativecommons.org/licenses/by-nc-sa/4.0/)

turístico que se comercializa. Sin embargo, los parámetros que intervienen en su diseño funcional no están muy bien establecidos y llegan a propiciar en muchos casos patrones de circulación en las corrientes que contribuyen a la erosión y la degradación de la costa. El presente trabajo forma parte del desarrollo del Sistema de Ingeniería Costera y Marítima (SICOM), que lleva a cabo el Centro de Investigaciones Hidráulicas de la Universidad Tecnológica de La Habana, centrado en simular tanto los cambios hidrodinámicos como morfológicos que ocurren en las playas cubanas ante la presencia de rompeolas sumergidos, y en obtener los parámetros de diseño para el empleo de estas obras en la mitigación de la erosión de las playas, utilizando modelos numéricos como herramientas predictivas.

Palabras clave: rompeolas sumergidos, cambios morfológicos, modelos numéricos.

Received: 05/22/2018

Accepted: 17/01/2021

Introduction

2022, Instituto Mexicano de Tecnología del Agua

Open Access bajo la licencia CC BY-NC-SA 4.0
(https://creativecommons.org/licenses/by-nc-sa/4.0/)

The coastal zone constitutes a resource of incalculable economic and social value that man has been using since ancient times and that has suffered in recent years a process of significant and generalized erosion, largely as a consequence of anthropic actions that interrupt the coastal transport of sediments and massive urbanism, among others. This problem is further accentuated in the context of Global Climate Change, in which numerous factors associated with atmospheric warming and rising mean sea levels have led to an increase in the incidence and intensity of storms that affect the geographical area, as well as the generalization of erosive problems, which entails great economic damage, the significant loss of spaces and extreme risks due to coastal flooding.

The need to implement solutions that guarantee the protection of the coastal zone, makes the use of submerged breakwaters be considered as a viable variant of application, since these works contribute to the conservation of the natural, aesthetic, and landscape conditions of the beaches, together at a lower economic cost by requiring less volume of materials. However, the parameters that intervene in its functional design are not very well established, so, if they are not correctly modeled and designed, they can promote circulation patterns in the currents that contribute to erosion and degradation of the coast (Ranasinghe, Larson, & Savioli, 2010).

In this sense, the work shows the application of the Coastal and Maritime Engineering System (SICOM), developed by the Hydraulic Research Center (Hernández & Córdova, 2015; Hernández & Córdova, 2016; Córdova, Hernández, & Benítez, 2017), focused on simulating both the hydrodynamic and morphological changes that occur on Cuban

2022, Instituto Mexicano de Tecnología del Agua

Open Access bajo la licencia CC BY-NC-SA 4.0
(https://creativecommons.org/licenses/by-nc-sa/4.0/)

beaches in the presence of submerged breakwaters, and on obtaining for the first time in the country, the design parameters for the use of these works in the mitigation of beach erosion, using the XBeach model (Roelvink *et al*., 2009), as it is capable of simulating both hydrodynamic and morphological processes in beaches, dune beaches and barrier beaches under high energy conditions. This model has been extended, applied, and validated by its authors with a series of analytical and laboratory cases and with field measurements in a large number of beaches bordering the regional seas of the European Union. As part of the work, the hydrodynamics of the model is previously calibrated and validated, using the results obtained from the physical modeling carried out in the laboratory of the University of Naples, Italy, for the case of the breakwater design in the traditional Havana seawall.

Materials and methods

The research design was carried out in two stages:

1. Calibration and validation of the XBeach model. The calibration and validation of the morphology of the model are reflected in Hernández and Córdova (2016), where the options break 1 is established as an energy dissipation model; as a gamma break index the value of 0.4; the

2022, Instituto Mexicano de Tecnología del Agua

Open Access bajo la licencia CC BY-NC-SA 4.0
(https://creativecommons.org/licenses/by-nc-sa/4.0/)

value of gammax 2 as the model limiter, and as the critical submerged slope wetslp the value of 0.3.

The hydrodynamics validation was carried out by reproducing with the XBeach the modeling carried out in the laboratory of the University of Naples as part of the campaign in physical models aimed at the design of breakwaters on the traditional Havana seawall. For this, the results obtained from the numerical modeling were compared with the values measured by the sensors in the wave tank of the physical model, where the characteristic profile of the traditional seawall was reproduced at 1:30 scale in a 1.56 m wide and 18.37 m long channel built inside the Random wave Tank (RATA). The experiments were carried out with two breakwaters, one with a wide crest with its freeboard at medium water level and the other with a narrow crest that emerges at 0.80 m. The coefficients of determination obtained were 0.86 for the significant wave heights and 0.97 for the wave setup, showing that the XBeach model is capable of correctly simulating the hydrodynamics that is generated in the presence of submerged breakwaters.

2. Establishment of the model and simulation of the hydrodynamic and morphological variables. A non-equidistant working mesh was established using profiles measured on the Varadero beach to which the equilibrium profile was determined using the expression given by García (2005) for the sediment scale parameter, which presents a better fit for characterizing the conditions of Cuban biogenic beaches (Figure 1). The mesh covers an area of 492 000 m^2 comprised by 615 m in a perpendicular direction to the coast with a resolution of 5 m (123 nodes) and 800 m along the coast with a resolution of 10 m (80 nodes), with

2022, Instituto Mexicano de Tecnología del Agua

Open Access bajo la licencia CC BY-NC-SA 4.0
(https://creativecommons.org/licenses/by-nc-sa/4.0/)

depths starting from the 8m isobath to reaching heights of 3 m above mean sea level in the dune area, which allowed us to visualize the processes that occurred in each simulation.

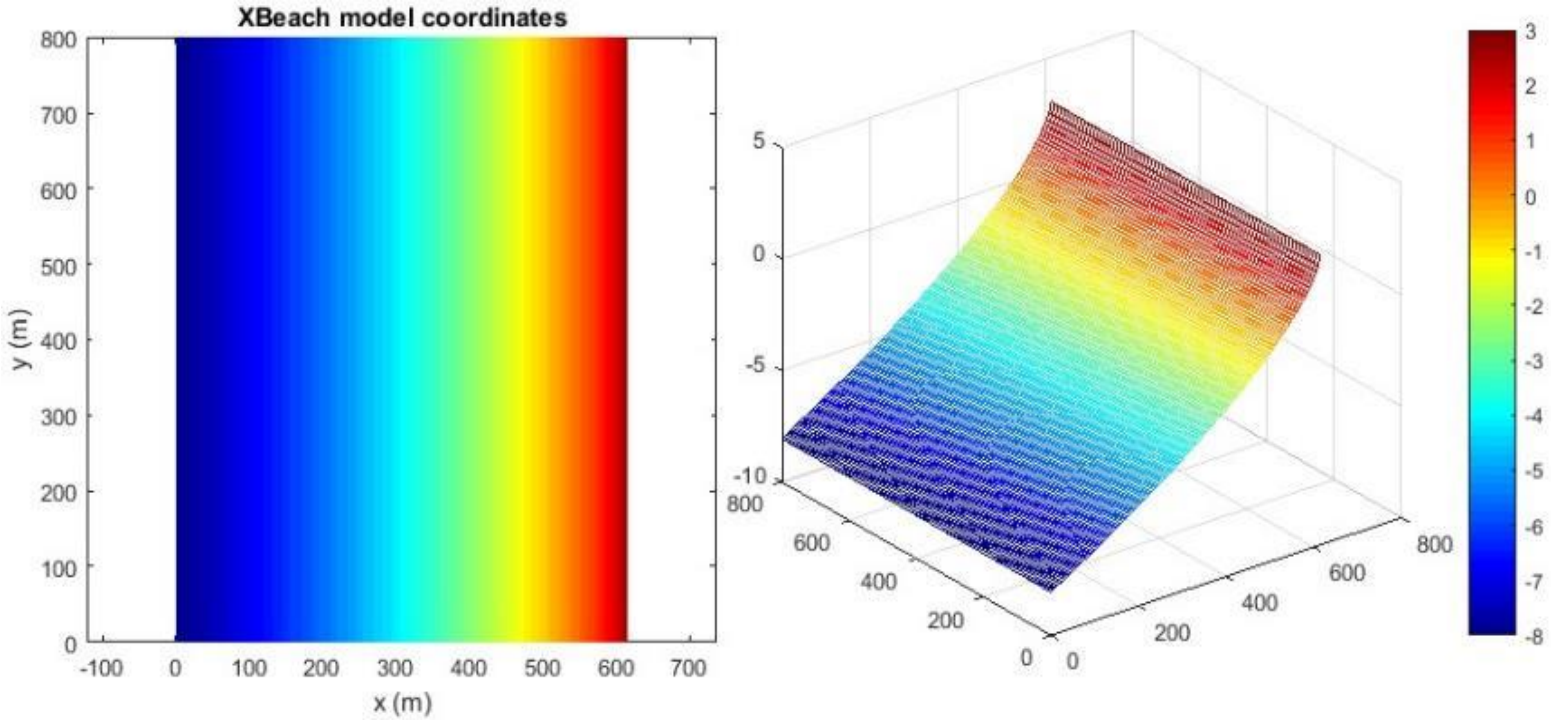

Figure 1. Working mesh. Source: Author's own.

Breakwaters were modeled both inside and outside the surge breaking zone. For the analysis, the values of 0.5 m, 1.5 m, and 2.5 m as significant wave heights with periods of 5.5 s and 6.5 s were selected, according to the data presented in the Global Wave Statistics for the geographic area that covers Cuba, Area 33, as observed in Table 1. Both the normal and oblique incidence of the waves is considered.

2022, Instituto Mexicano de Tecnología del Agua

Open Access bajo la licencia CC BY-NC-SA 4.0
(https://creativecommons.org/licenses/by-nc-sa/4.0/)

Table 1. Wave height and studied periods. Source: Global Wave Statistic, Area 33.

Hs (m)								
8,5				1	1			
7,5			1	1	1	1		
6,5		1	2	3	2	1		
5,5		1	5	6	5	2	1	
4,5		4	12	15	10	4	2	
3,5	2	13	31	32	49	7	2	1
2,5	6	37	70	59	29	10	3	1
1,5	22	90	49	74	28	7	2	0
0,5	56	96	66	25	6	1	0	0
Tm(s)	4,5	5,5	6,5	7,5	8,5	9,5	10,5	11,5

The hydrodynamic and morphological variables studied are reflected in Table 2. The simulations were carried out by varying the variables to know the changes that are generated on the beach, for a total of 440 variants analyzed.

2022, Instituto Mexicano de Tecnología del Agua

Open Access bajo la licencia CC BY-NC-SA 4.0
(https://creativecommons.org/licenses/by-nc-sa/4.0/)

Table 2. Hydrodynamic and morphological variables to study. Source: Author's own.

Variables	Description	Units
Hydrodynamics		
Hs	Significant wave height (0.5, 1.5, 2.5)	m
Tm	Mean wave period (5.5, 6.5)	s
ϴ	Wave incidence angle (90, 315)	°
Breakwater geometry		
Lb	Length (100, 200, 300)	m
Wb	Crest wight (10, 20)	m
Sb	Submergence (-0.00, -0.50, -1.00)	m
Xb	Distance to the coast (30, 60, 90, 120, 150, 180, 210, 240, 270, 300)	m
Physical		
m	Submerged beach slope (0.025)	-
D_{50}	Mean sediment diameter (0.26)	mm
ω	Fall velocity (4.49)	cm/s
γs	Specific weight of sediment (2.716)	kg/cm^3

Results

2022, Instituto Mexicano de Tecnología del Agua

Open Access bajo la licencia CC BY-NC-SA 4.0
(https://creativecommons.org/licenses/by-nc-sa/4.0/)

Effect of the length of the submerged breakwater (*Lb*)

The most relevant results obtained from the modeling of the hydrodynamic, breakwater geometric, and physical variables are presented.

In Figure 2 you can see from left to right, the representation of the simulations referring to breakwaters of lengths of 100 m, 200 m, and 300 m respectively, with a crest width of 10 m and submergence -0.5 m, located 60 m from the coastline. The profiles where there is greater interest for analysis were defined, which are:

- Profile 41: Profile that passes through the center of the breakwater in all variants, being called a profile with the presence of breakwaters.
- Profile 16: Profile that passes through an area far from the breakwater and the border of the working mesh, called profile without the presence of breakwater.

2022, Instituto Mexicano de Tecnología del Agua

Open Access bajo la licencia CC BY-NC-SA 4.0
(https://creativecommons.org/licenses/by-nc-sa/4.0/)

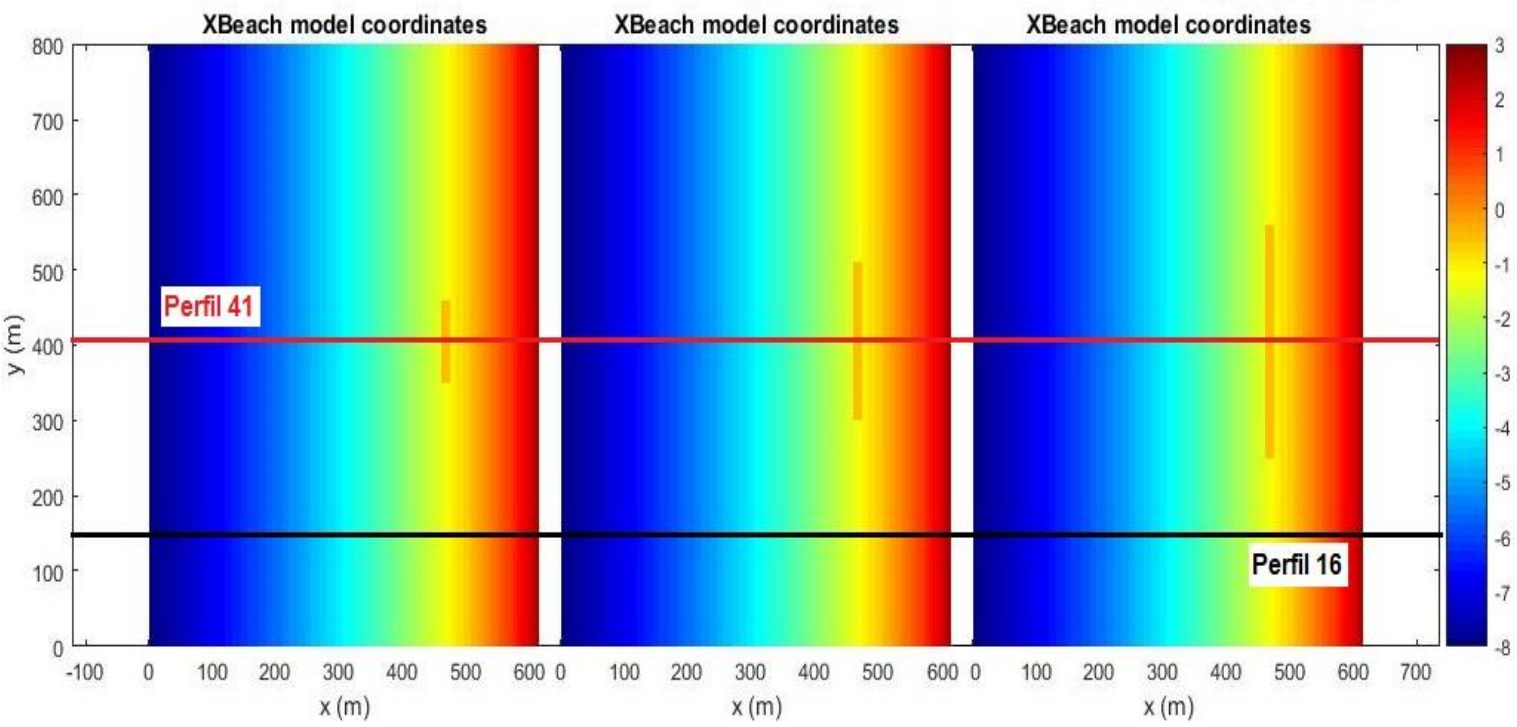

Figure 2. Representation of the working mesh with the breakwaters located at 60 m and waves incident perpendicular to the coast. Source: Author's own.

The influence exerted by the breakwater on the mean square height of the gravity waves can be assessed qualitatively and quantitatively in Figure 3 and Table 3, observing how after interacting with the breakwater its values decrease in all variants. It is also seen that the transmission coefficient, which relates the transmitted and incident wave heights, presents very similar values in the three variants, although the length of the breakwater varies.

2022, Instituto Mexicano de Tecnología del Agua

Open Access bajo la licencia CC BY-NC-SA 4.0
(https://creativecommons.org/licenses/by-nc-sa/4.0/)

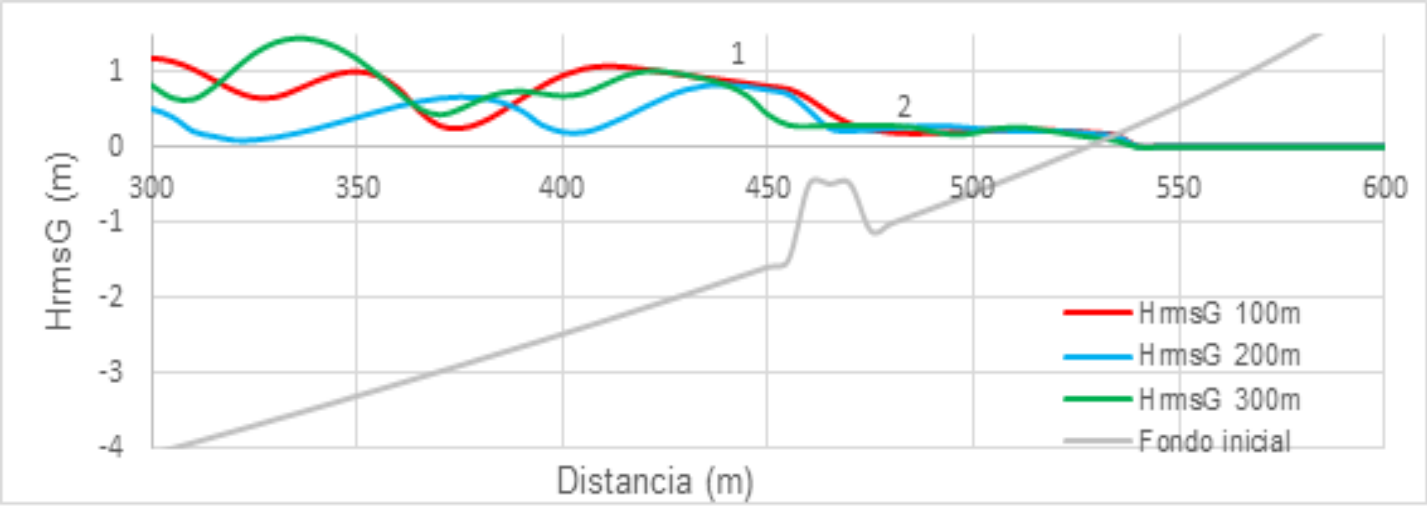

Figure 3. Representation of the mean square height of gravity waves for breakwaters of 100 m, 200 m, and 300 m in length located 60 m from the coast. Source: Author's own.

Table 3. Transmission analysis as a function of breakwater length. Source: Author's own.

Variants	Length (m)	HrmsG (m)		Kt
		Point 1	Point 2	
2	100	0,7826	0,2466	0,32
122	200	0,7140	0,2288	0,32
212	300	0,7801	0,2397	0,31

Notice: Points 1 and 2 are located to 5 m towards the sea and toward the coast of the crest of the breakwater respectively.

2022, Instituto Mexicano de Tecnología del Agua

Open Access bajo la licencia CC BY-NC-SA 4.0
(https://creativecommons.org/licenses/by-nc-sa/4.0/)

Table 4 shows the mean square height of the gravity waves in Profile 16, without the presence of breakwaters, and in Profile 41 with the presence of breakwaters, where the effectiveness of the breakwater can be verified by attenuating the energy of the incident wave and the percentage of dissipation that it guarantees.

Table 4. Mean square wave height of gravity waves in profile 16 and profile 41. Source: Author's own.

Variants	Length (m)	HrmsG (m)		Dissipation (%)
		Point 2 Profile 16	Point 2 Profile 41	
2	100	0,6428	0,2466	61,63
122	200	0,5437	0,2288	57,91
212	300	0,5168	0,2397	53,61

When interacting with the breakwater, the speed reached by the flow increases as a result of the strong turbulence that is generated, being greater for the breakwater that is 100 m long (Figure 4).

2022, Instituto Mexicano de Tecnología del Agua

Open Access bajo la licencia CC BY-NC-SA 4.0
(https://creativecommons.org/licenses/by-nc-sa/4.0/)

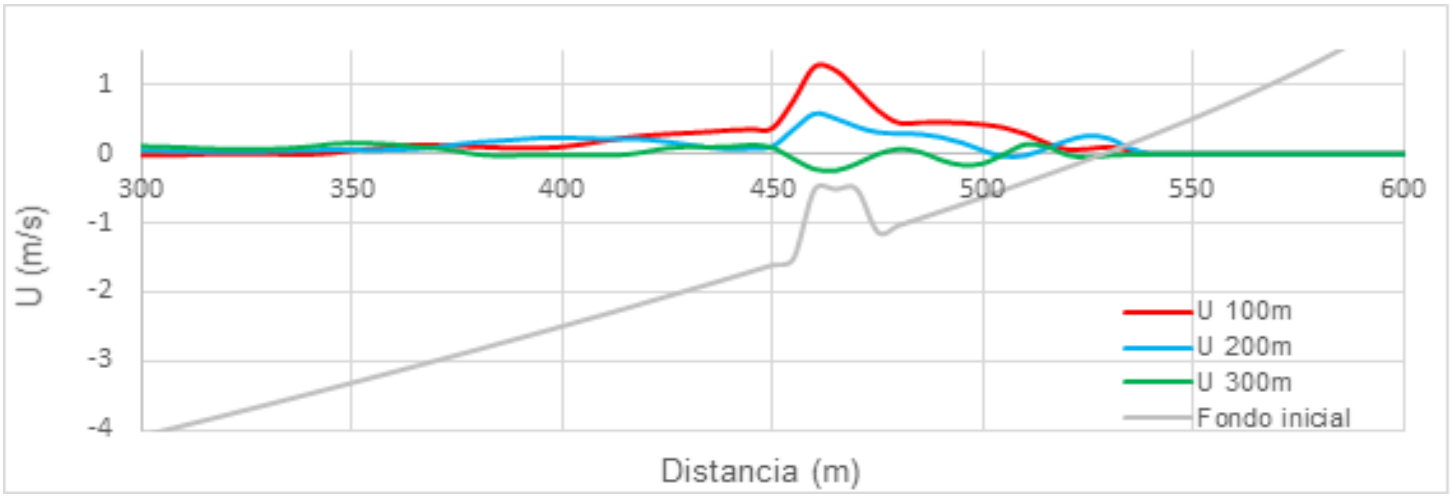

Figure 4. Flow velocities for the breakwater are located 60 m from the coastline with lengths of 100 m, 200 m, and 300 m. Source: Author's own.

The flow patterns are shown in Figure 5, which resemble the two-cell erosive pattern described by Ranasinghe *et al*. (2010), where the red line indicates the initial position of the coast. Although the behavior of currents and, therefore, how the bottom changes are similar in all three variants, the zone of influence increases the longer the breakwater length.

2022, Instituto Mexicano de Tecnología del Agua

Open Access bajo la licencia CC BY-NC-SA 4.0
(https://creativecommons.org/licenses/by-nc-sa/4.0/)

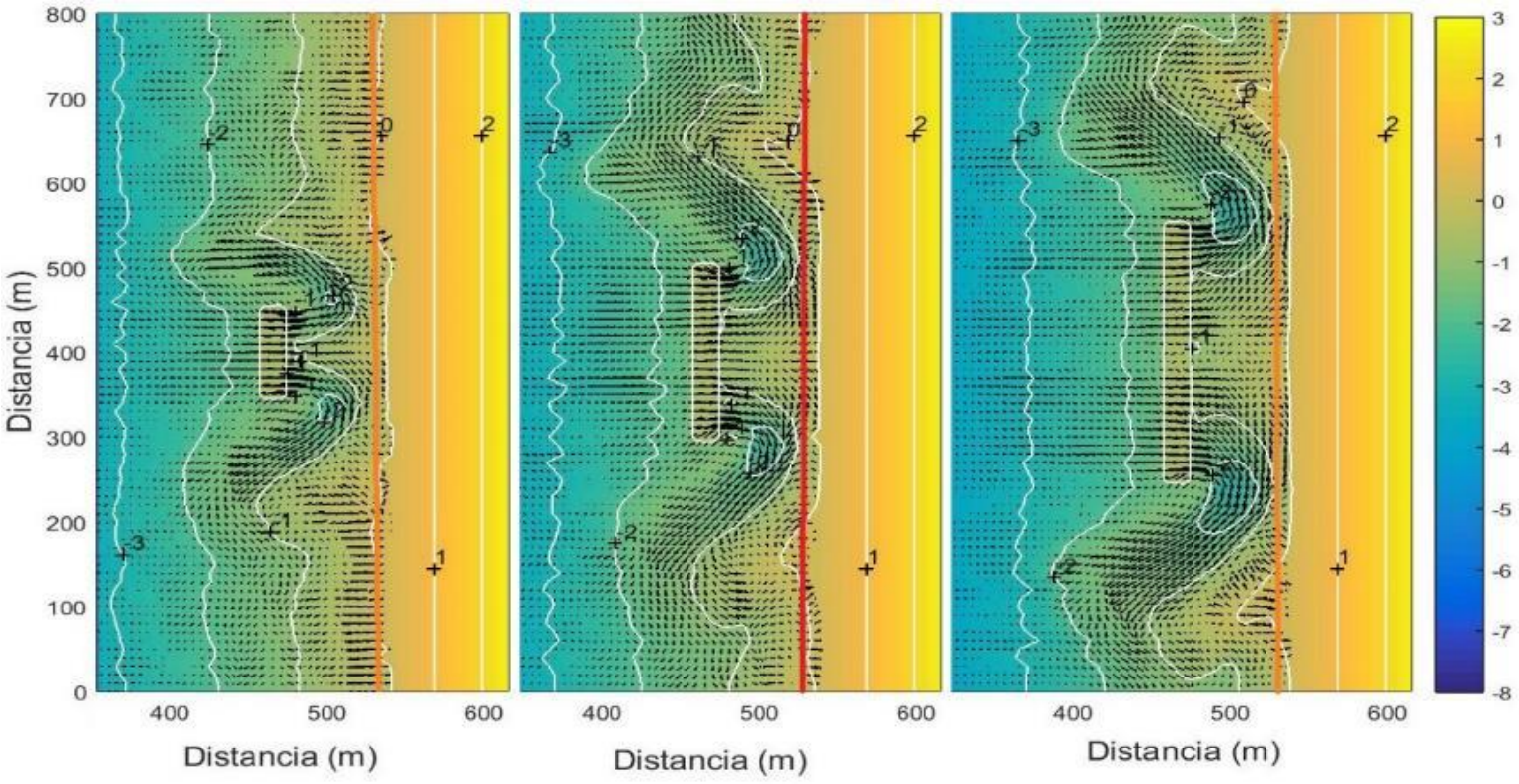

Figure 5. Representation of flow patterns and bottom variation for breakwaters located 60 m from the coast. Source: Author's own.

Figure 6 reveals how the value of the wave setup increases after the interaction with the breakwater. Comparing the setup around the coastline, it is noted how this variable decreases in the three variants analyzed just in the center of the sheltered zone, where Profile 41 transits. Table 5 shows the setup in Profile 16 without the presence of breakwaters and in Profile 41 with the presence of breakwaters, both for point 1 located 5 m after the breakwater crest has been surpassed, and for point 2 located on the coastline. In it, it can be seen how in Profile 16 the values of the setup at point 2 when reaching the coast are higher than for the variant

2022, Instituto Mexicano de Tecnología del Agua

Open Access bajo la licencia CC BY-NC-SA 4.0
(https://creativecommons.org/licenses/by-nc-sa/4.0/)

with breakwaters, which can be seen in Figure 6, where the red line represents the initial position of the coast.

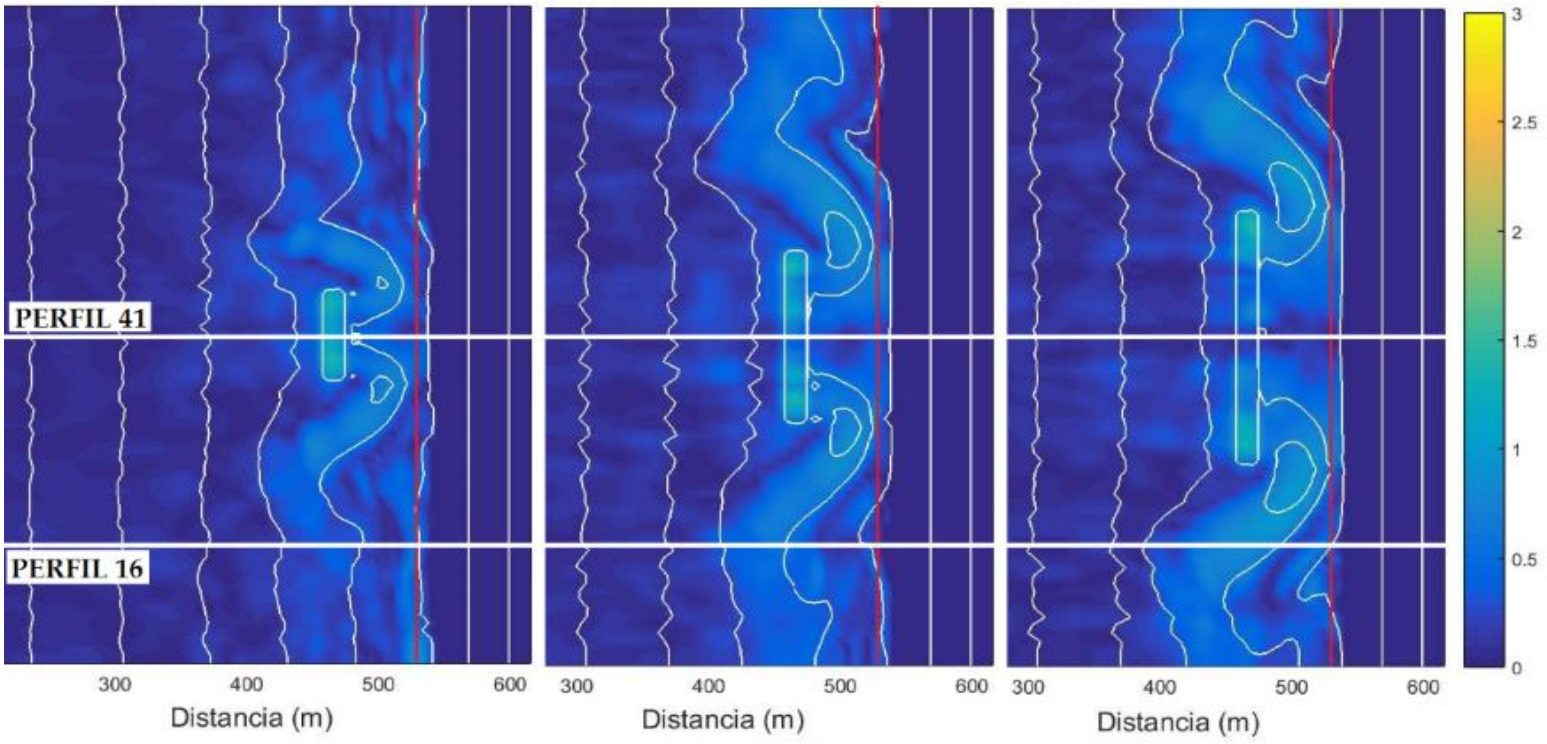

Figure 6. Representation of the setup Zs for the breakwaters located 60 m from the coast with lengths of 100 m, 200 m, and 300 m. Source: Author's own.

Table 5. Wave setup in Profile 16 and Profile 41. Source: Author's own.

Variants	Length (m)	Profile 16		Profile 41	
		Point 1	Point 2	Point 1	Point 2
2	100	0,1133	0,2283	0,1101	0,1709

2022, Instituto Mexicano de Tecnología del Agua

Open Access bajo la licencia CC BY-NC-SA 4.0
(https://creativecommons.org/licenses/by-nc-sa/4.0/)

122	200	0,1447	0,1899	0,1271	0,1803
212	300	0,0413	0,2430	0,1049	0,1484

The red line in Figure 7 shows the position of the coast before the location of the breakwater, attesting to the morphological changes suffered by the bottom and the erosive process that occurred. The currents generated by the presence of the breakwater, transport the sediments found in the sheltered area out to sea, creating at its end's areas of greater depth and the erosion of the coastline throughout the beachfront. The formation of scour at the ends of the breakwater shelter area can affect their stability causing abrupt failure and coincides with the research developed in physical models by (Papadopoulos, 2012).

2022, Instituto Mexicano de Tecnología del Agua

Open Access bajo la licencia CC BY-NC-SA 4.0
(https://creativecommons.org/licenses/by-nc-sa/4.0/)

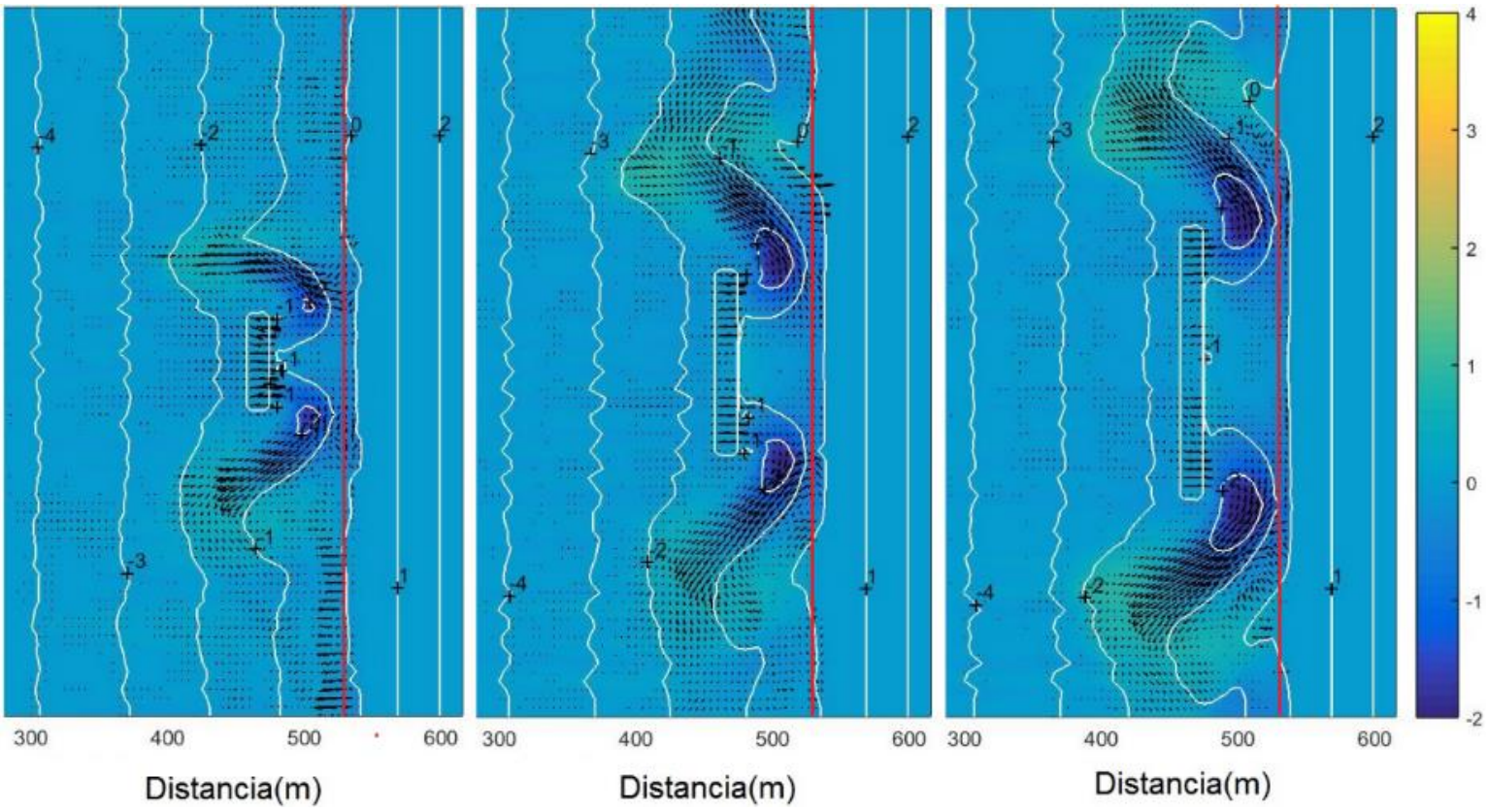

Figure 7. Representation of sediment transport and bottom variation. Source: Author's own.

The resulting profile that passes through the center of the breakwater for the analyzed variants, shows the morphological evolution of the seabed, where the coastline presents sediment loss and retreat, as seen in Figure 8. For the 100 m long breakwater, the profile undergoes a greater erosive process, which is associated with the speeds reached by the currents.

2022, Instituto Mexicano de Tecnología del Agua

Open Access bajo la licencia CC BY-NC-SA 4.0
(https://creativecommons.org/licenses/by-nc-sa/4.0/)

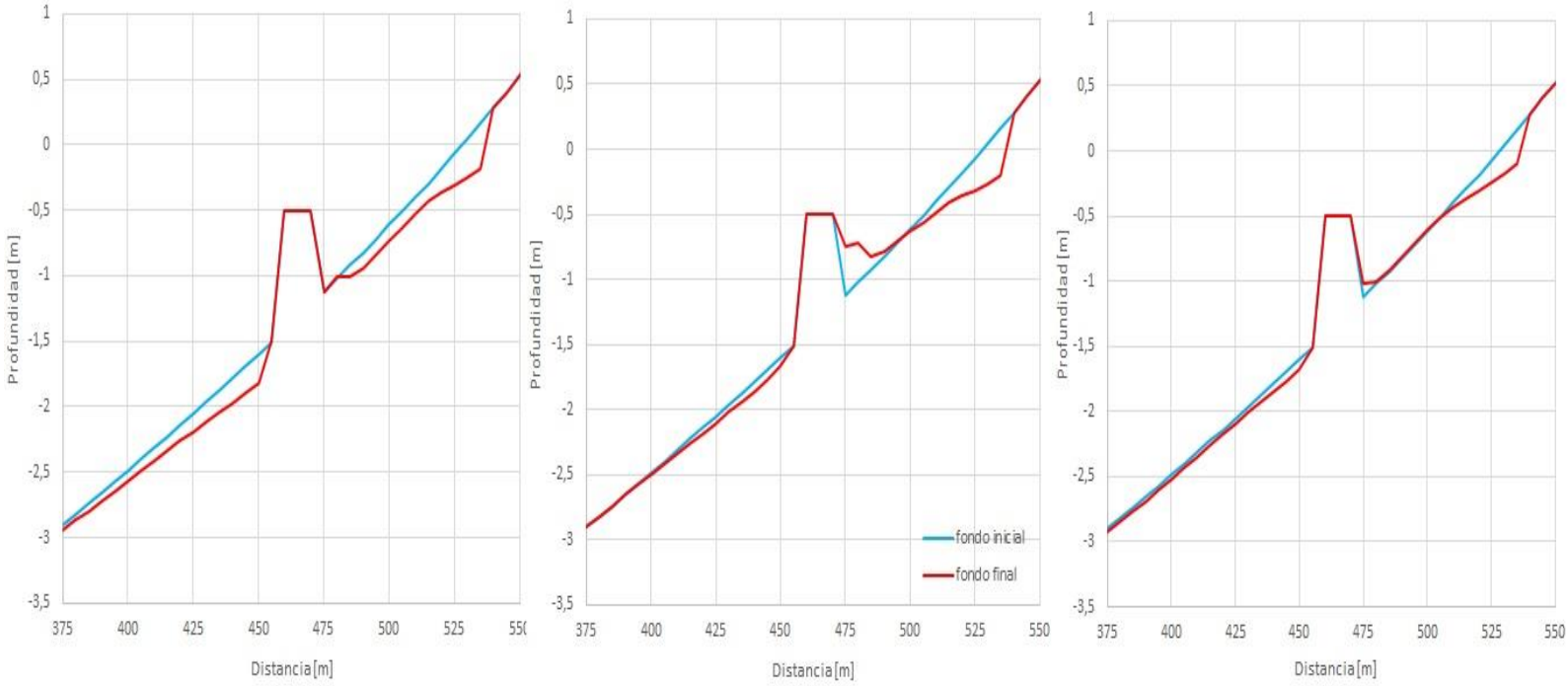

Figure 8. Evolution of the seabed for breakwaters of 100 m (left), 200 m (center), and 300 m long (right). Source: Author's own.

Effect of the crest width (Wb)

Figure 9 shows the simulations of breakwaters of 100 m, 200 m, and 300 m in length, with a crest width of 20 m and submergence -0.5 m, located at 60 m with waves incident perpendicular to the coast. Table 6 shows the mean square wave height of the gravity waves obtained. Its values

2022, Instituto Mexicano de Tecnología del Agua

Open Access bajo la licencia CC BY-NC-SA 4.0
(https://creativecommons.org/licenses/by-nc-sa/4.0/)

prove that the transmission coefficient is lower compared to the 10 m wide variants, being the breakwater more effective in dissipating the wave height, which coincides with the study of Makris and Memos (2007).

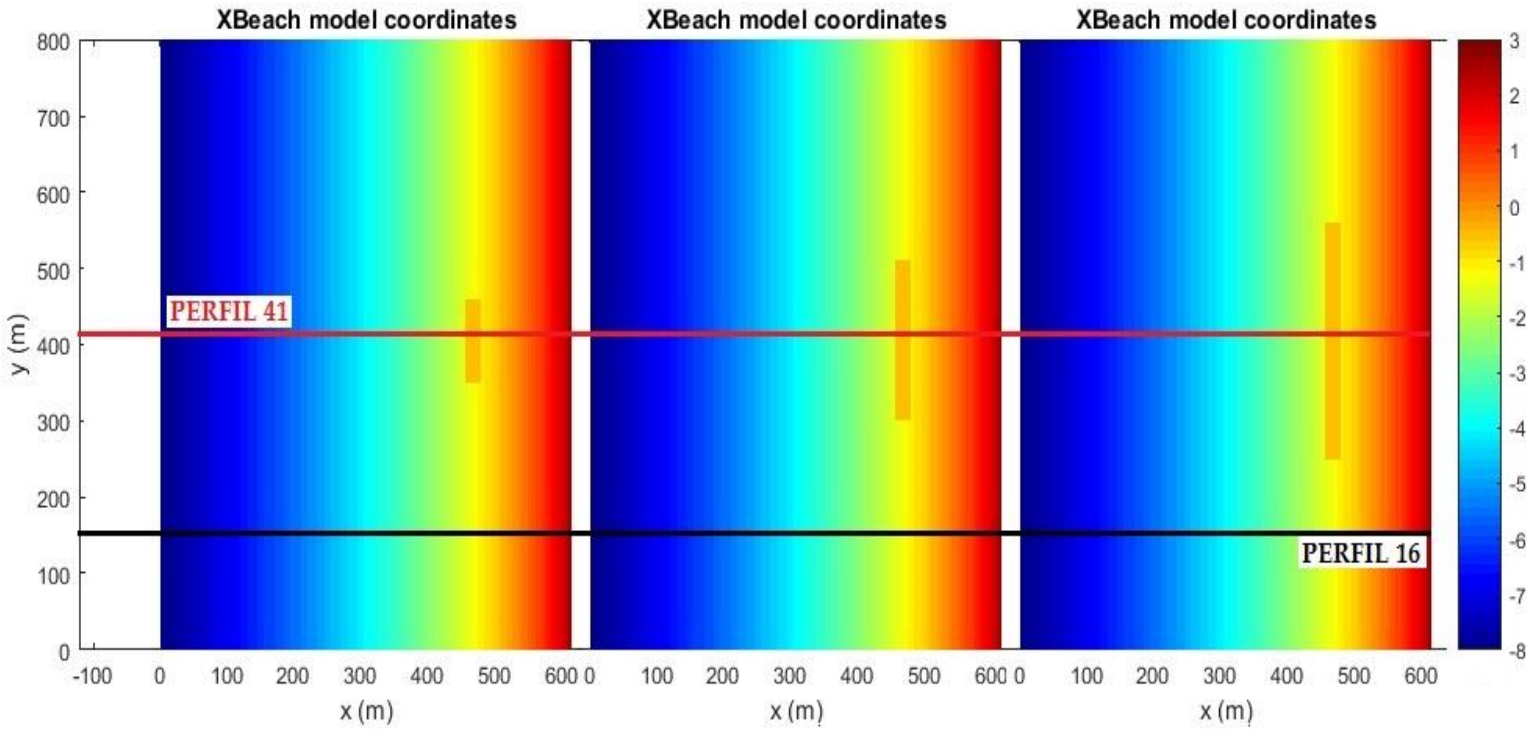

Figure 9. Working mesh with breakwaters of 20 m crest width and lengths of 100 m, 200 m, and 300 m located 60 m from the coast. Source: Author's own.

Table 6. Analysis of the transmission as a function of the crest width of the breakwater. Source: Author's own.

Variants			**Hrms (m)**	**Kt**

2022, Instituto Mexicano de Tecnología del Agua

Open Access bajo la licencia CC BY-NC-SA 4.0
(https://creativecommons.org/licenses/by-nc-sa/4.0/)

	Length (m)	Width of breakwaters (m)	Punto 1	Punto 2	
2	100	10	0,7826	0,2466	0,32
92		20	0,8183	0,2197	0,27
122	200	10	0,7140	0,2288	0,32
392		20	0,7867	0,2172	0,28
212	300	10	0,7801	0,2397	0,31
402		20	0,8055	0,2177	0,27

Note: Points 1 and 2 are located 5 m towards the sea and the coast of the breakwater crest respectively.

Figure 10 reflects the relationship of the dimensionless parameter Wb / Hi and the transmission coefficient Kt, for the breakwaters of 100 m, 200 m, and 300 m in length located in the different positions studied. As can be seen, the highest transmission coefficient values correspond to breakwaters with a crest width of 10 m, while they decrease significantly for breakwaters that are 20 m wide.

2022, Instituto Mexicano de Tecnología del Agua

Open Access bajo la licencia CC BY-NC-SA 4.0
(https://creativecommons.org/licenses/by-nc-sa/4.0/)

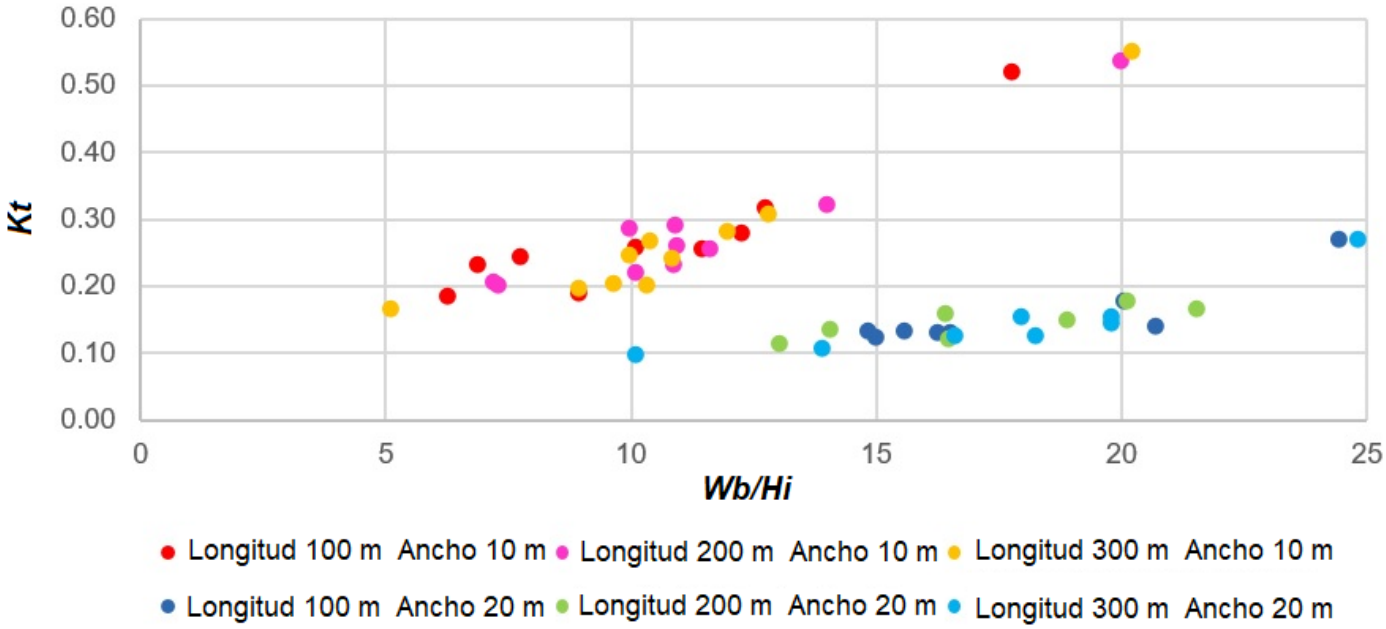

Figure 10. Relationship between the dimensionless parameter (Wb / Hi) and the transmission coefficient Kt, for breakwaters of 10 m and 20 m wide. Source: Author's own.

Table 7 can observe the speed of the flow reached by the waves in their interaction with the breakwater. When comparing the variants with widths of 10 m and 20 m, it is appreciated how it is greater for the latter, due to the turbulence that is generated by the increase in wave breakage.

Table 7. Flow velocities when interacting (Point 1) and after interacting with the breakwater (Point 2). Source: Author's own.

Variants	Length (m)		Speed (m/s)

2022, Instituto Mexicano de Tecnología del Agua

Open Access bajo la licencia CC BY-NC-SA 4.0
(https://creativecommons.org/licenses/by-nc-sa/4.0/)

		Width of breakwaters (m)	Punto 1	Punto 2
2	100	10	1,2546	0,4467
92		20	1,6576	0,5511
122	200	10	0,5803	0,3137
392		20	0,6180	0,4264
212	300	10	0,2050	0,1299
402		20	0,4631	0,1204

Regarding the flow and circulation patterns of the currents, the analyzed variants are erosive in nature. In Figure 11 these patterns are observed, with the retreat of the coastline for both the 10 m wide crest breakwater and the 20 m wide breakwater, with the latter being more pronounced, where the red line represents the initial position of the coast.

2022, Instituto Mexicano de Tecnología del Agua

Open Access bajo la licencia CC BY-NC-SA 4.0
(https://creativecommons.org/licenses/by-nc-sa/4.0/)

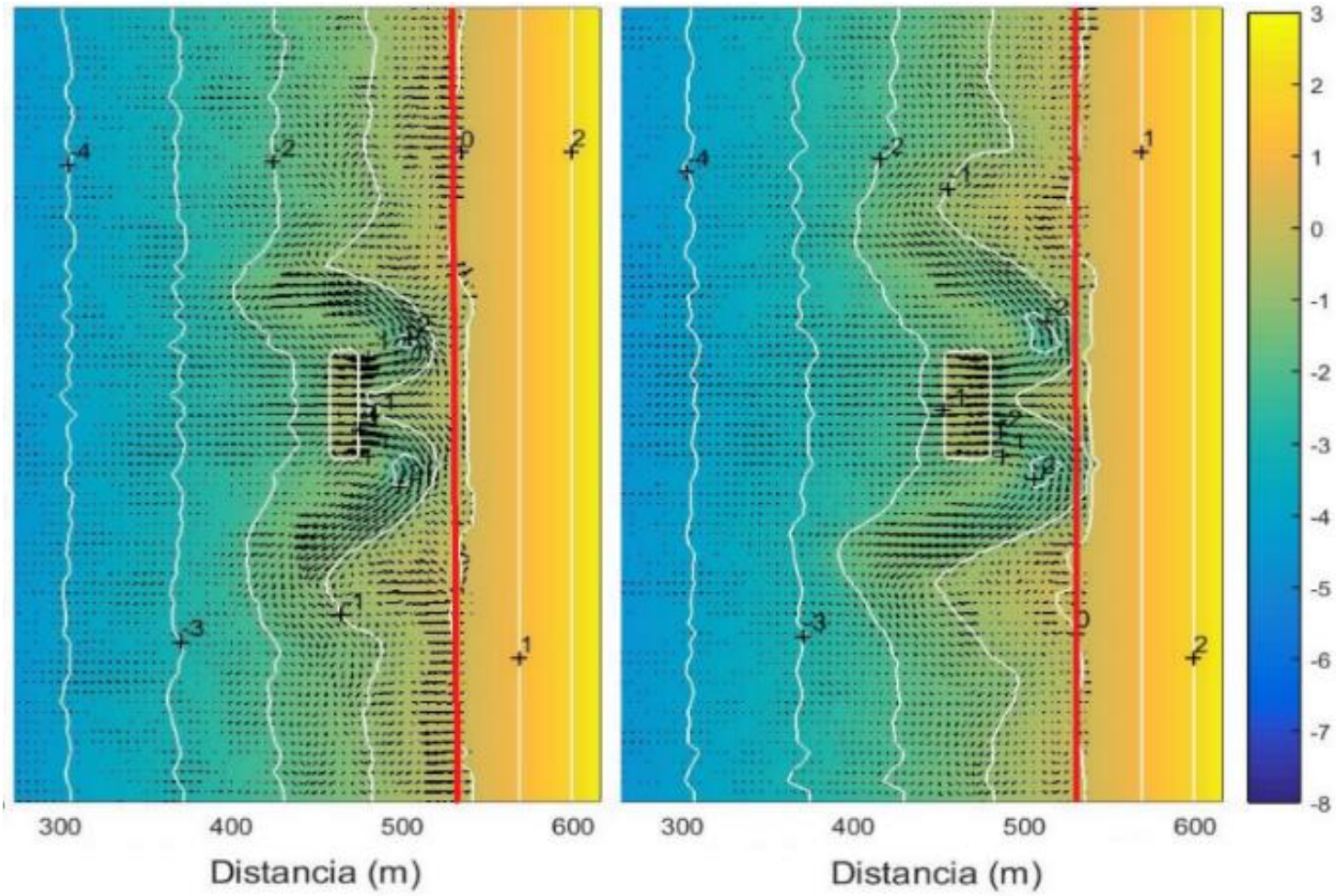

Figure 11. Current circulation patterns for the 100 m long breakwater located 60 m from the coast. Left: variant 10 m wide. Right: variant 20 m wide. Source: Author's own.

Table 8 shows the surge elevation in Profile 16 without the presence of breakwaters and in Profile 41 with the presence of breakwaters, both for point 1 located 5 m from the crest of the breakwater and at point 2 located on the coastline, corresponding to breakwaters 20 m wide. When comparing the values with those given in Table 5 for the 10 m wide

2022, Instituto Mexicano de Tecnología del Agua

Open Access bajo la licencia CC BY-NC-SA 4.0
(https://creativecommons.org/licenses/by-nc-sa/4.0/)

breakwaters, it is observed how the sea-level rise on the coastline increases, which can be seen in Figure 12.

Table 8. Sea level rise in Profile 16 and Profile 41 for breakwaters of 20 m wide crest. Source: Author's own.

Variants	Length (m)	Profile 16		Profile 41	
		Punto 1	Punto 2	Punto 1	Punto 2
92	100	0,0857	0,1899	0,1756	0,2129
392	200	0,1628	0,2066	0,1429	0,1951
402	300	0,1244	0,2052	0,2409	0,1676

2022, Instituto Mexicano de Tecnología del Agua

Open Access bajo la licencia CC BY-NC-SA 4.0
(https://creativecommons.org/licenses/by-nc-sa/4.0/)

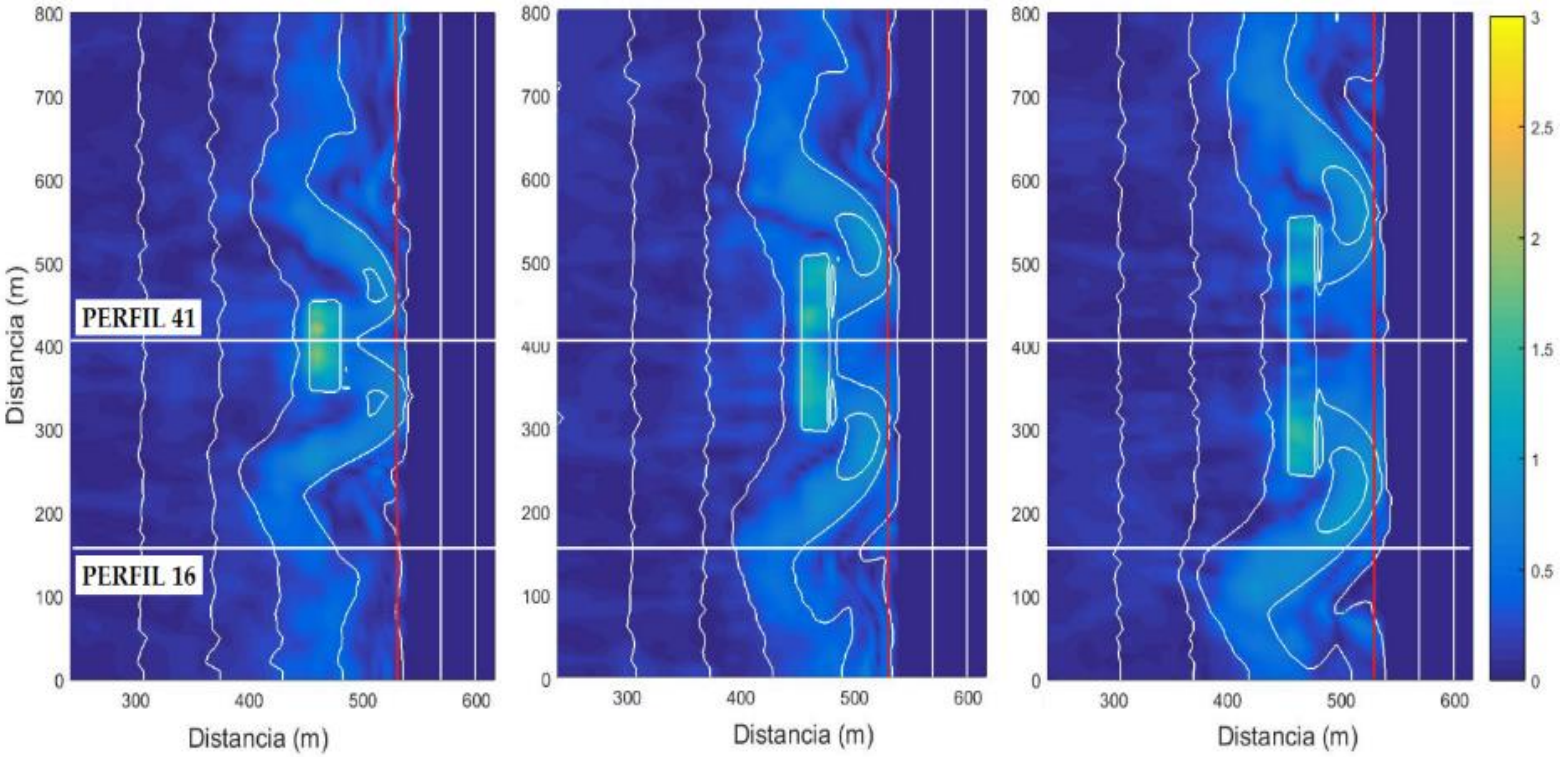

Figure 12. Wave setup for 20 m wide breakwaters located 60 m from the coast with lengths of 100 m, 200 m, and 300 m. Source: Author's own.

When observing the behavior of Profile 41, which passes through the center of the 100 m long breakwater, the morphological evolution of the seabed is noted, where the coastline presents loss of sediment and retreat, as seen in Figure 13. For the 20 m wide breakwater, there is marked erosion throughout the profile, which intensifies at its base due to increased flow velocities, which could cause the failure of the structure.

2022, Instituto Mexicano de Tecnología del Agua

Open Access bajo la licencia CC BY-NC-SA 4.0
(https://creativecommons.org/licenses/by-nc-sa/4.0/)

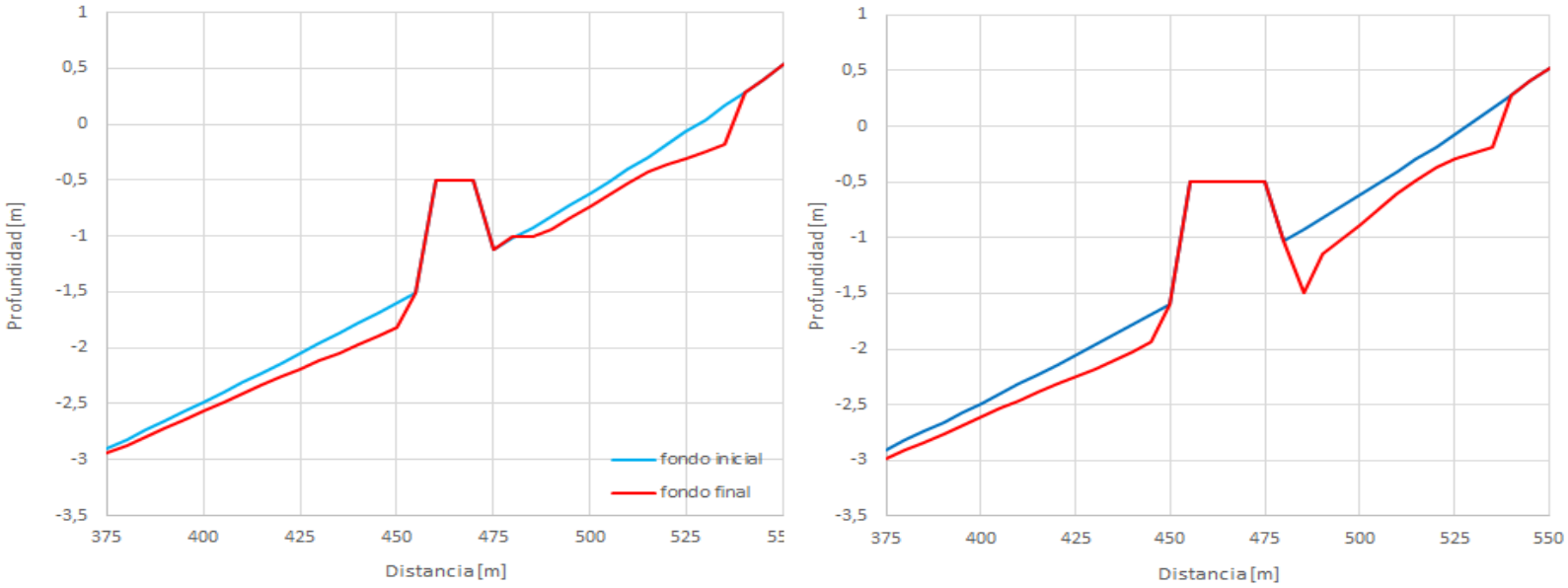

Figure 13. The behavior of the bottom. Right: Breakwater 10 m wide. Left: Breakwater 20 m wide. Source: Author's own.

Effect of submergence (Sb)

The effect of submergence is observed through the transmission coefficient in Figure 14, where for 0.00 m submergence breakwaters the values decrease until very close to zero while they increase with the increase in submergence until reaching values of 0.54 for breakwaters with the submergence of -1.00 m.

2022, Instituto Mexicano de Tecnología del Agua

Open Access bajo la licencia CC BY-NC-SA 4.0
(https://creativecommons.org/licenses/by-nc-sa/4.0/)

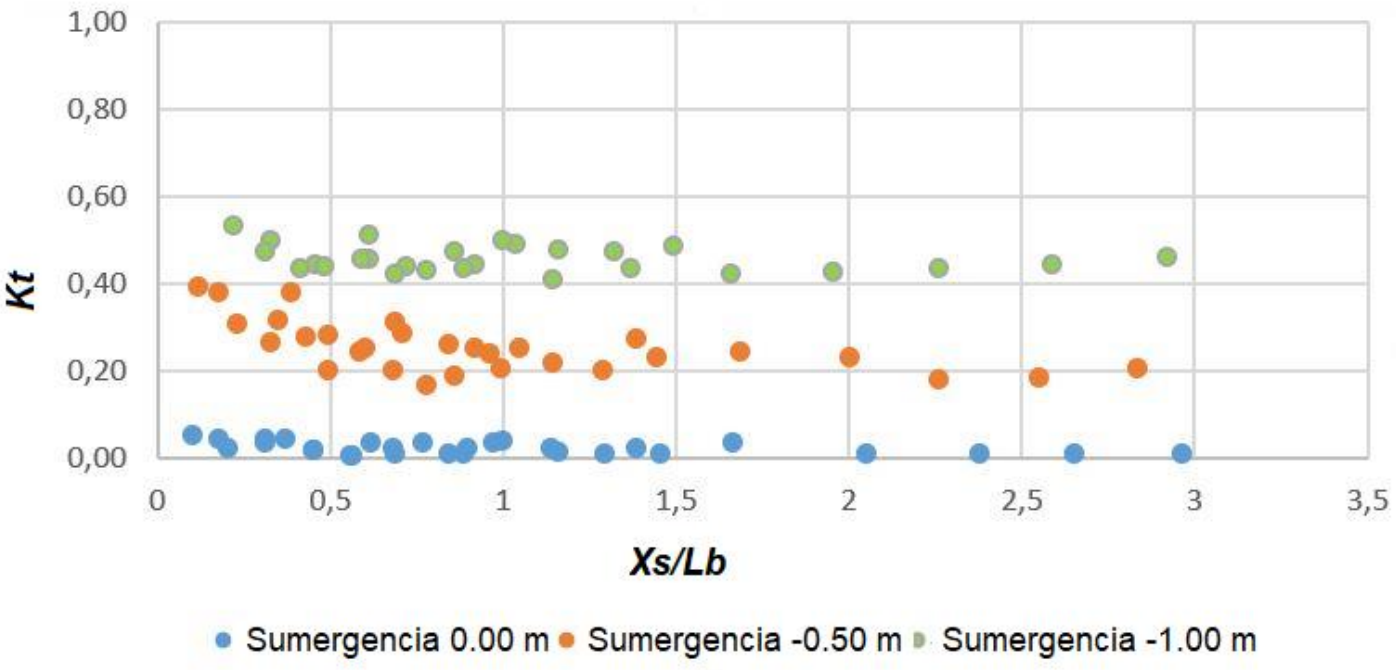

Figure 14. Effects of submergence on the transmission coefficient. Source: Author's own.

Figure 15 reflects the sediment transport generated by the presence of the breakwater located 120 m from the coast with the submergence of 0.00 m, -0.50 m, and -1.00 m, where its effect on the beach decreases as submergence increases, which was pointed out by (Calabrese, Vicinanza, & Buccino, 2008) and verified by Ranasinghe *et al*. (2010).

2022, Instituto Mexicano de Tecnología del Agua

Open Access bajo la licencia CC BY-NC-SA 4.0
(https://creativecommons.org/licenses/by-nc-sa/4.0/)

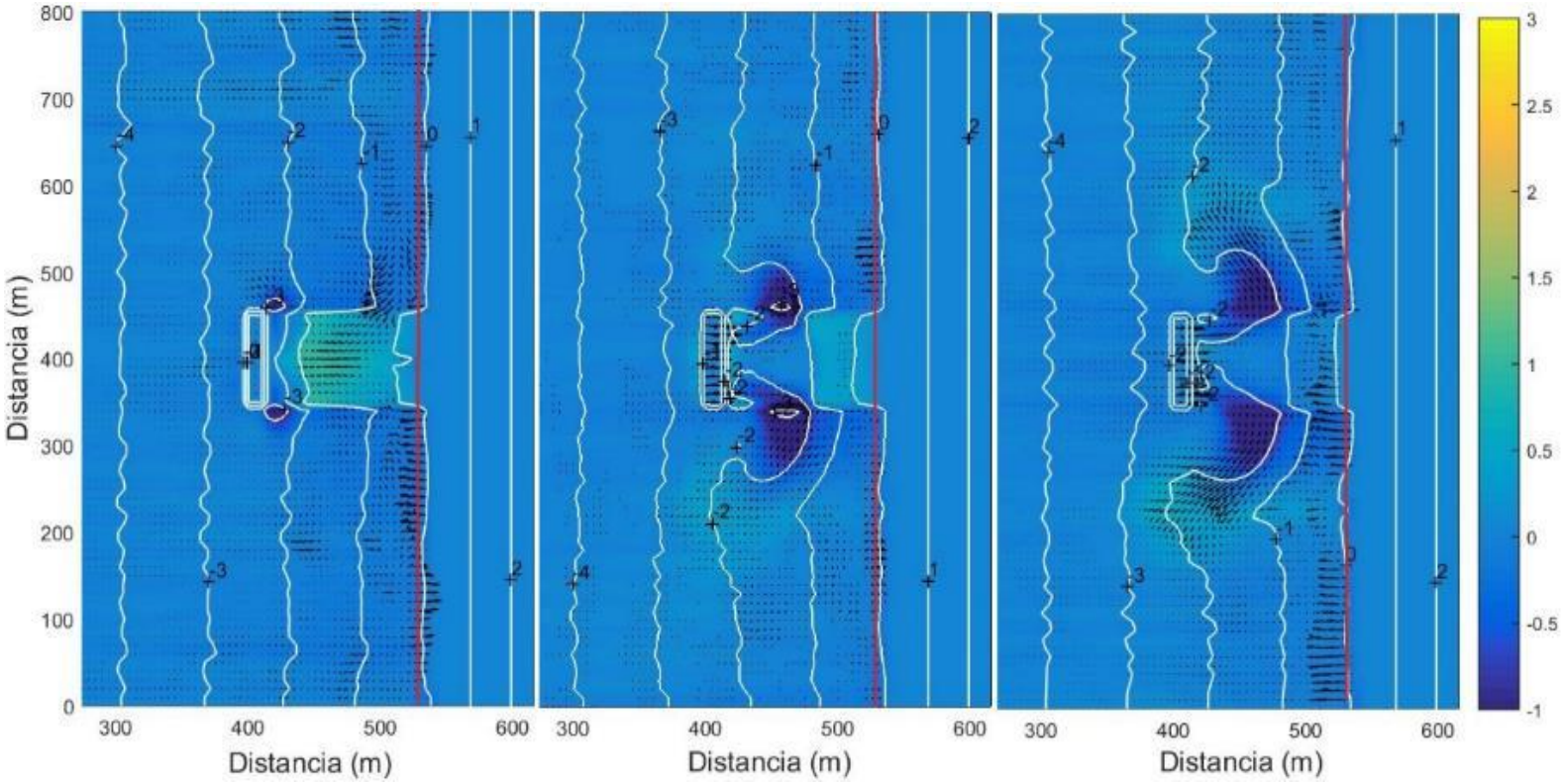

Figure 15. Sediment transport. Left: Submergence 0.00 m. Center: Submergence -0.50 m. Right: Submergence -1.00 m. Source: Author's own.

Effect of wave obliquity (ϴ)

The modeling carried out under the oblique influence of the waves, experience a behavior similar to that obtained under the waves acting

2022, Instituto Mexicano de Tecnología del Agua

Open Access bajo la licencia CC BY-NC-SA 4.0
(https://creativecommons.org/licenses/by-nc-sa/4.0/)

perpendicular to the coast, which coincides with the investigations carried out by Vanlishout (2008) and with the proposals of Ranasinghe *et al*. (2010). Table 9 and Table 10 show the transmission coefficients and wave setup for breakwaters located 60 m from the coast with 100 m, 200 m, and 300 m in length under the oblique action of the waves, which can be compared with Tables 3 and 6 where the waves act perpendicular to the coast.

Table 9. Analysis of the transmission according to the incidence of the waves. Breakwaters with a crown width of 10 m and submergence of -0.50 m. Source: Author's own.

Variants	Length (m)	HrmsG (m)		Kt
		Punto 1	Punto 2	
302	100	0.7864	0.2399	0.31
332	200	0.5452	0.1680	0.31
362	300	0.7879	0.2466	0.31

Table 10. Wave setup values. 10 m crown width breakwaters and -0.50 m submergence. Source: Author's own.

Variants	Length (m)	Profile 16		Profile 41	
		Punto 1	Punto 2	Punto 1	Punto 2
302	100	0.1241	0.2329	0.1038	0.1899

2022, Instituto Mexicano de Tecnología del Agua

Open Access bajo la licencia CC BY-NC-SA 4.0
(https://creativecommons.org/licenses/by-nc-sa/4.0/)

332	200	0.1130	0.1923	0.1219	0.1733
362	300	0.0532	0.2312	0.1148	0.1609

The patterns of flow and circulation of the currents present a behavior similar to that observed for the waves acting normal to the coast, with the retreat of the coastline for the nearby locations, as shown in Figure 16. The morphological evolution of the seabed under the oblique incidence of the waves can be observed in Figure 17, where the coastline presents a behavior very similar to that obtained under the waves acting perpendicular to the coast, with loss of sediment and retreat, which shows that the obliquity of the waves does not exert significant influence in coastal response mode.

2022, Instituto Mexicano de Tecnología del Agua

Open Access bajo la licencia CC BY-NC-SA 4.0
(https://creativecommons.org/licenses/by-nc-sa/4.0/)

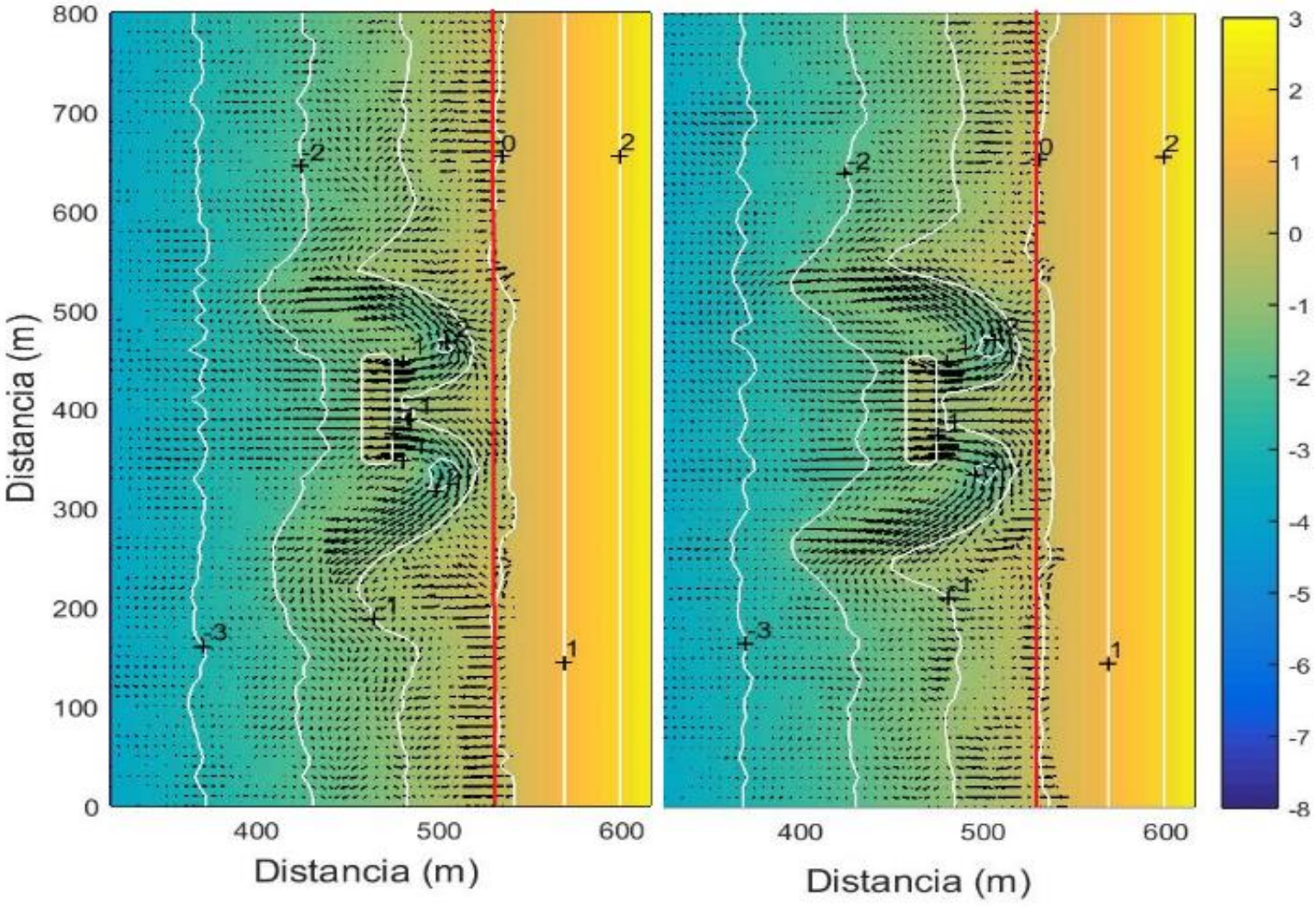

Figure 16. Current patterns for breakwaters 100 m long and 10 m wide are located 60 m from the coast with a -0.5 m submergence. Left: Perpendicular swell. Right: Oblique swell. Source: Author's own.

2022, Instituto Mexicano de Tecnología del Agua

Open Access bajo la licencia CC BY-NC-SA 4.0
(https://creativecommons.org/licenses/by-nc-sa/4.0/)

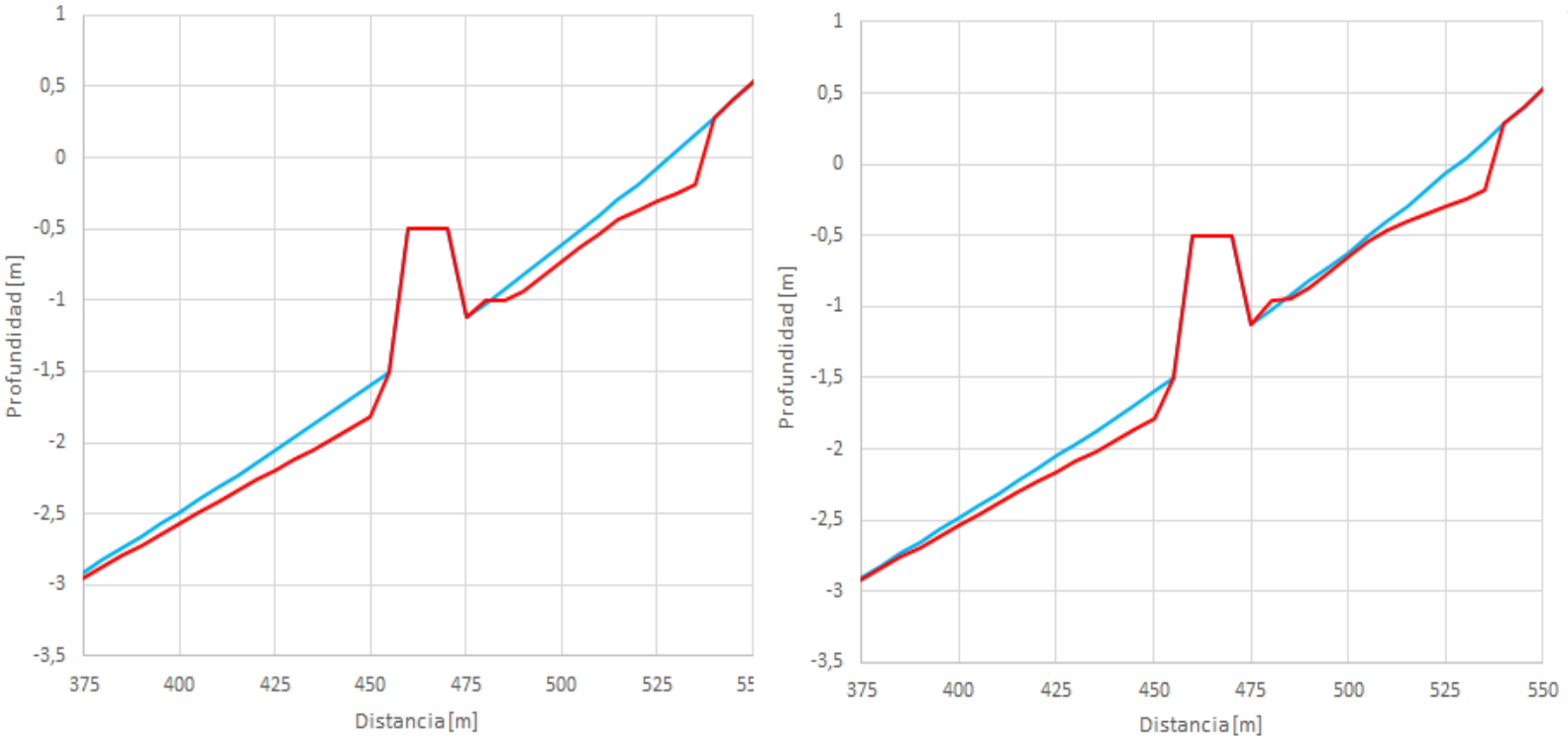

Figure 17. Evolution of the seabed for breakwaters 100 m long and 10 m wide located 60 m from the coast with the submergence of -0.5 m. Left: Perpendicular swell. Right: Oblique swell. Source: Author's own.

Effect of the distance to the coast of the submerged breakwater (*Xb*)

2022, Instituto Mexicano de Tecnología del Agua

Open Access bajo la licencia CC BY-NC-SA 4.0
(https://creativecommons.org/licenses/by-nc-sa/4.0/)

The analysis was carried out by varying the distances to the coastline, locating the breakwaters at 30, 60, 90, 120, 150, 180, 210, 240, 270, and 300 m apart. The effect of the breakwater placement distance on the mean square height of gravity waves and on the transmission, coefficient is shown in Figure 18, which decreases as the breakwater moves away from the coast, corresponding to the lowest values in all the cases to the 20 m wide breakwaters.

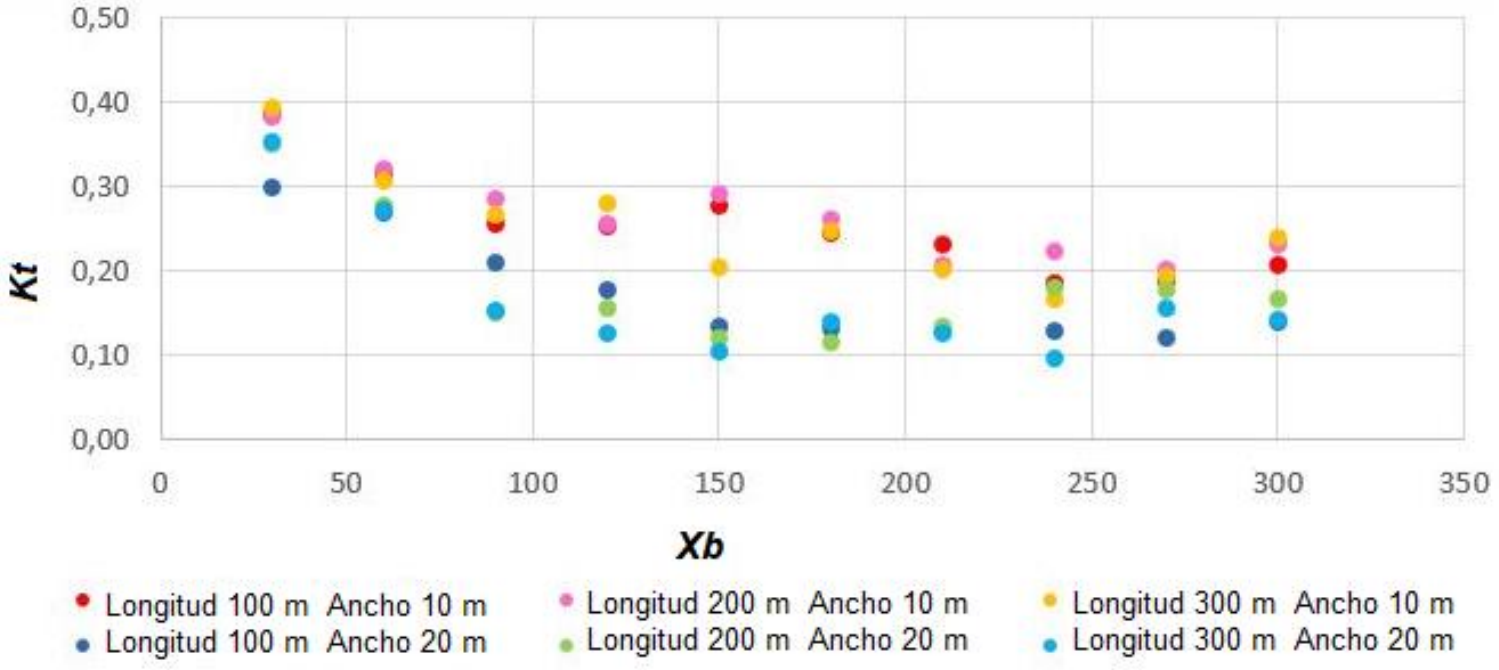

Figure 18. Transmission coefficient as a function of the breakwater placement distance from the coast for breakwaters of 100 m, 200 m, and 300 m in length and a crest width of 10 m and 20 m.

2022, Instituto Mexicano de Tecnología del Agua

Open Access bajo la licencia CC BY-NC-SA 4.0
(https://creativecommons.org/licenses/by-nc-sa/4.0/)

Figure 19 reflects the speed and circulation patterns of the currents for the nearshore locations, where erosive two-cell patterns occur. As the breakwater moves away from the coast, cumulative patterns of four cells begin to appear and an advance of the coastline concerning its initial position, highlighted by the red line, behaviors described by (Ranasinghe, Larson, & Savioli, 2010).

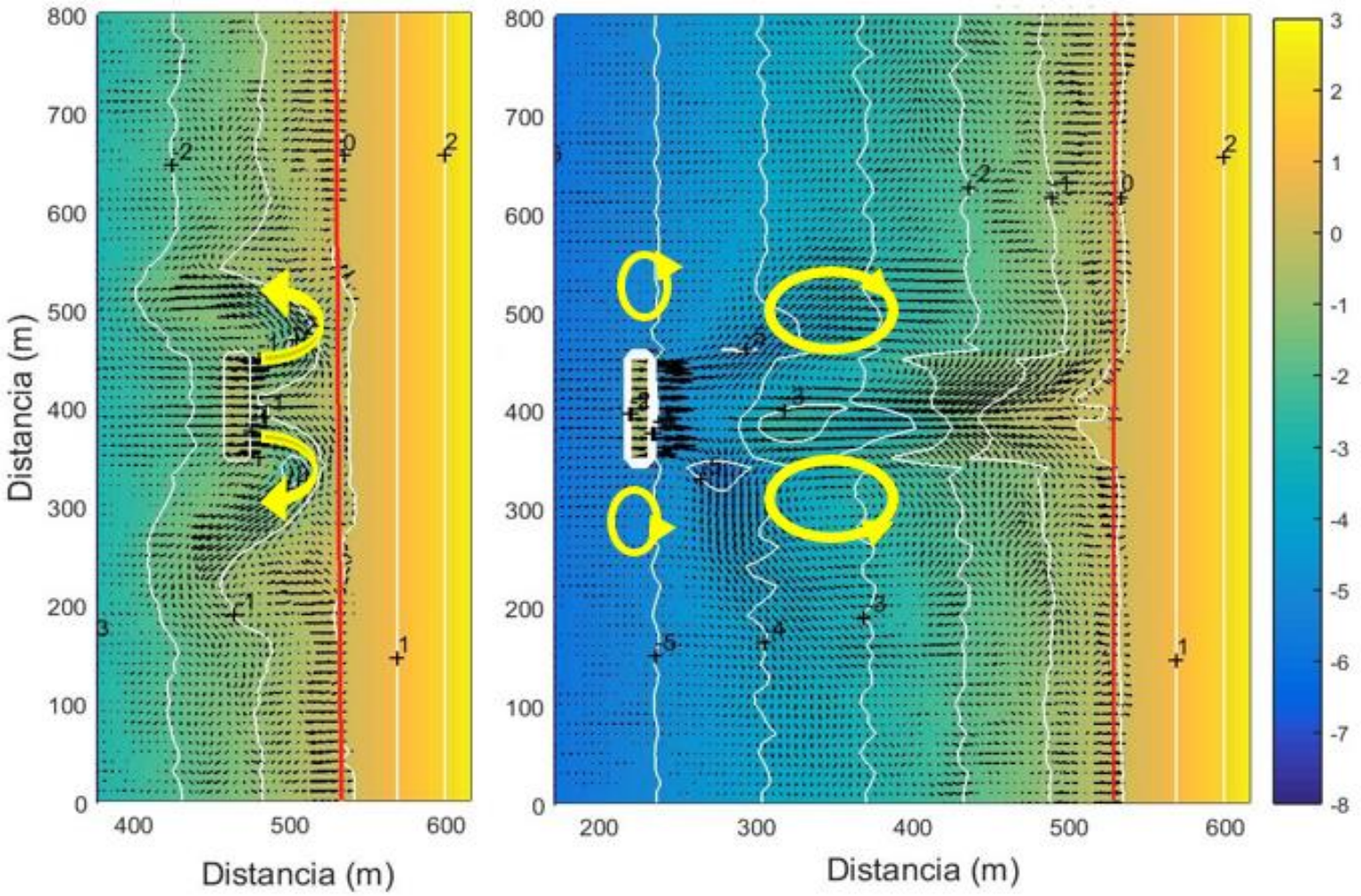

2022, Instituto Mexicano de Tecnología del Agua

Open Access bajo la licencia CC BY-NC-SA 4.0
(https://creativecommons.org/licenses/by-nc-sa/4.0/)

Figure 19. Circulation of currents. Left: Breakwater 90 m away and erosive two-cell patterns. Right: Breakwater 300 m away and cumulative four-cell patterns. Source: Author's own.

The behavior of the flow velocity patterns is confirmed in the representation of the sediment transport given in Figure 20, which agrees with the morphological changes suffered by the bottom and with the position adopted by the coastline. The evolution of the seabed over time is reflected in Figure 21, where the left image, corresponding to the breakwater located 90 m from the coast, shows the erosion suffered by the beach while the right image, for the breakwater, is located 300 m away from the coast, it shows the accumulation of sediments and the progress achieved.

2022, Instituto Mexicano de Tecnología del Agua

Open Access bajo la licencia CC BY-NC-SA 4.0
(https://creativecommons.org/licenses/by-nc-sa/4.0/)

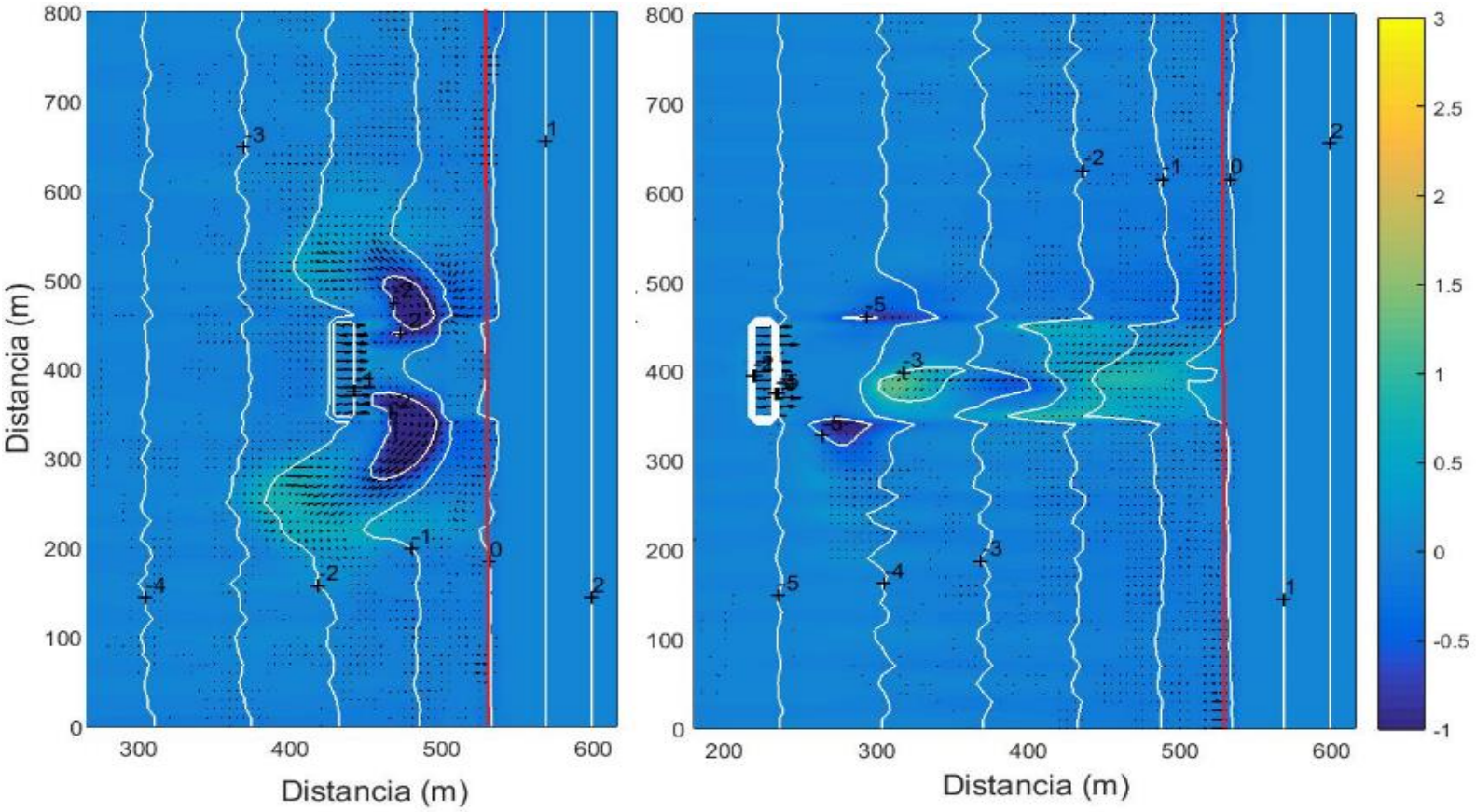

Figure 20. Sediment transport for breakwaters 10 m wide. Left breakwater 90 m away from the coast and right 300 m. Source: Author's own.

2022, Instituto Mexicano de Tecnología del Agua

Open Access bajo la licencia CC BY-NC-SA 4.0
(https://creativecommons.org/licenses/by-nc-sa/4.0/)

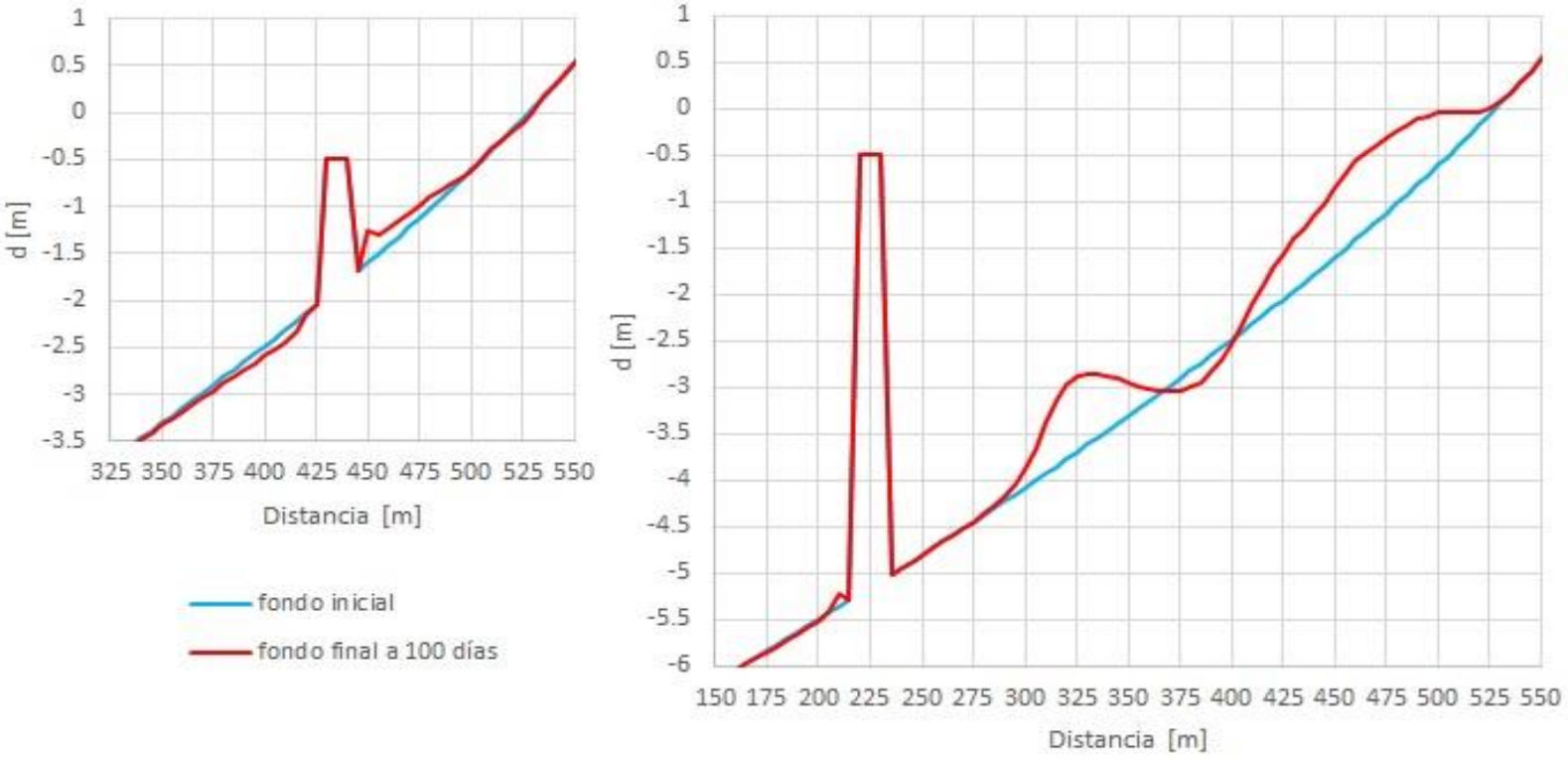

Figure 21. The behavior of the bottom for breakwaters of 10 m wide crest located 90 m from the coast (left) and 300 m (right). Source: Author's own.

Figure 22 indicates the results of the movement of the coastline (erosion/accretion) obtained depending on the location of the breakwater, both for waves with incidence perpendicular to the coast and for waves with oblique incidence.

2022, Instituto Mexicano de Tecnología del Agua

Open Access bajo la licencia CC BY-NC-SA 4.0
(https://creativecommons.org/licenses/by-nc-sa/4.0/)

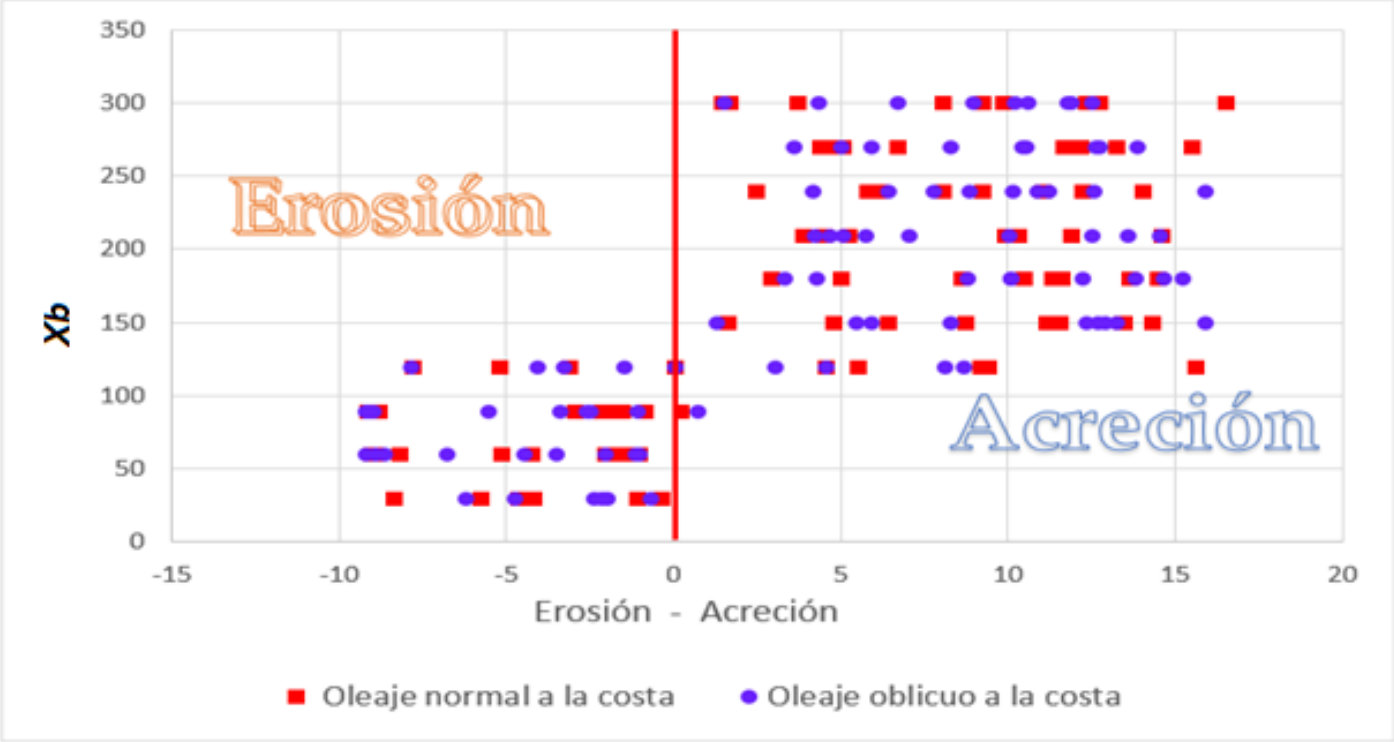

Figure 22. Response of the shoreline (erosion/accretion) as a function of the breakwater placement distance. Source: Author's own.

Figure 23 shows how for near positions up to 100 m away, the coastline recedes in all the studied breakwater lengths, which is highlighted with a red box. From the 120 m separation of the breakwater from the coast, advances in the coastline begin to be observed, although erosive processes are also manifested, behaving as a transition zone (green box). For positions greater than 150 m there is always an accumulation of sediments on the beach, which can reach up to 18 m in width and are delimited in yellow.

2022, Instituto Mexicano de Tecnología del Agua

Open Access bajo la licencia CC BY-NC-SA 4.0
(https://creativecommons.org/licenses/by-nc-sa/4.0/)

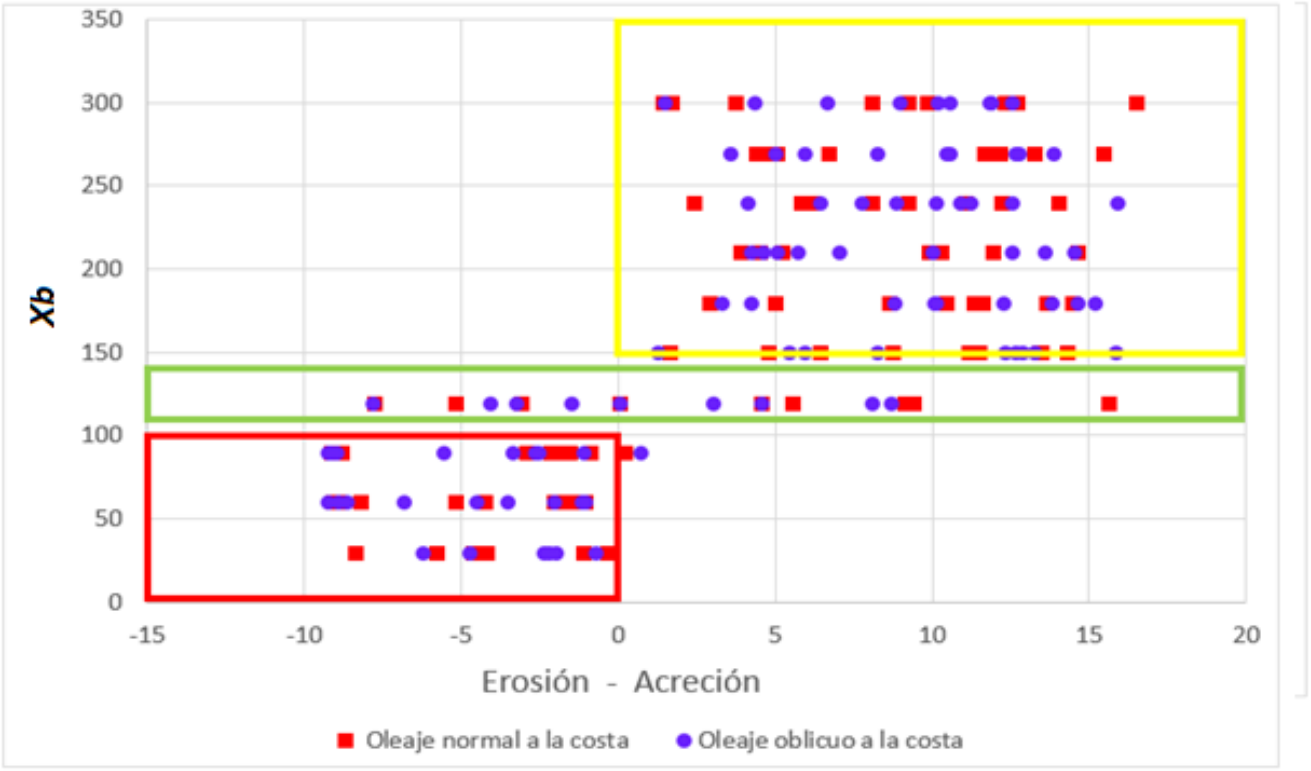

Figure 23. Response of the coast (erosion/accretion) as a function of the breakwater placement distance and its delimitation. Source: Author's own.

The simulations varying the distance from the breakwater to the coast, show the presence of erosive two-cell circulation patterns or cumulative four-cell patterns, this being one of the dominant parameters that determine the coastal response mode.

Figure 24, Figure 25, and Figure 26 show the morphological response of the beach through the length of the shaped spit (*Xs*), which varies depending on the length of the breakwater (*Lb*) and the distance

2022, Instituto Mexicano de Tecnología del Agua

Open Access bajo la licencia CC BY-NC-SA 4.0
(https://creativecommons.org/licenses/by-nc-sa/4.0/)

concerning the original coast (*Xb*), through the dimensionless parameter *Lb*/*Xb*, which constitute the main design parameters that govern the functional behavior of these works.

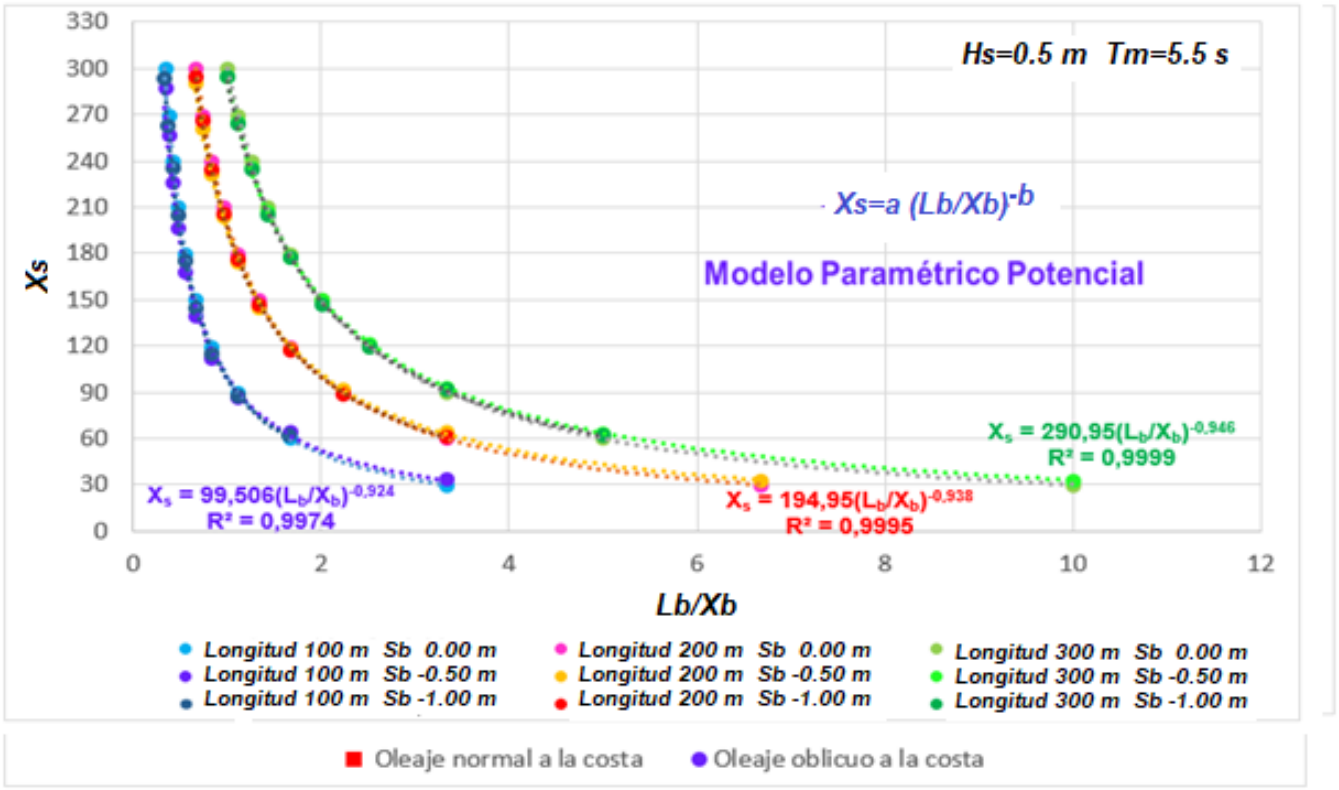

Figure 24. Relationship Length of breakwater/initial distance to shore *vs*. distance to resulting shoreline (*Xs*). *Hs* = 0.5 m, *Tm* = 5.5 s. Source: Author's own.

Tecnología y Ciencias del Agua

2022, Instituto Mexicano de Tecnología del Agua

Open Access bajo la licencia CC BY-NC-SA 4.0
(https://creativecommons.org/licenses/by-nc-sa/4.0/)

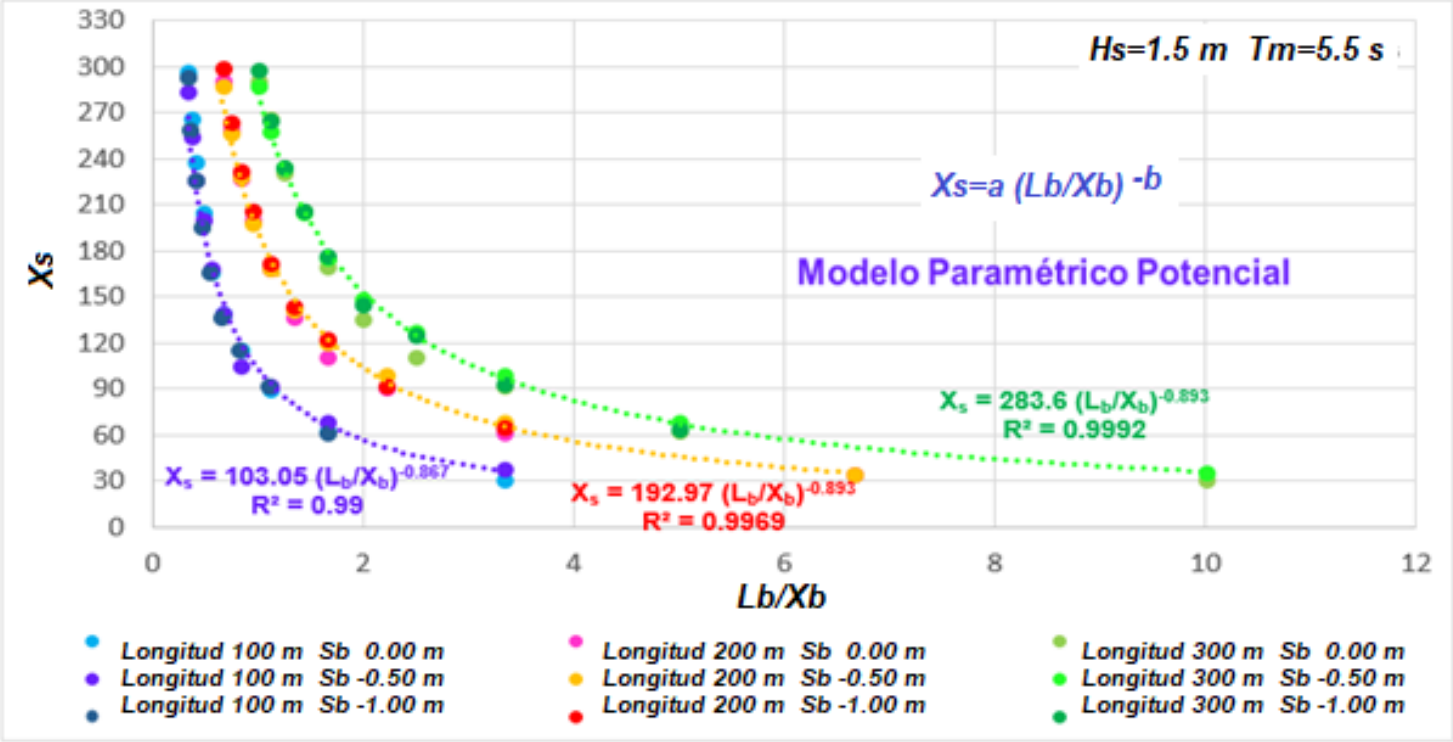

Figure 25. Relationship Length of breakwater / Initial distance to shore *vs*. distance to resulting shoreline (*Xs*). *Hs* = 1.5 m, *Tm* = 5.5 s. Source: Author's own.

2022, Instituto Mexicano de Tecnología del Agua

Open Access bajo la licencia CC BY-NC-SA 4.0
(https://creativecommons.org/licenses/by-nc-sa/4.0/)

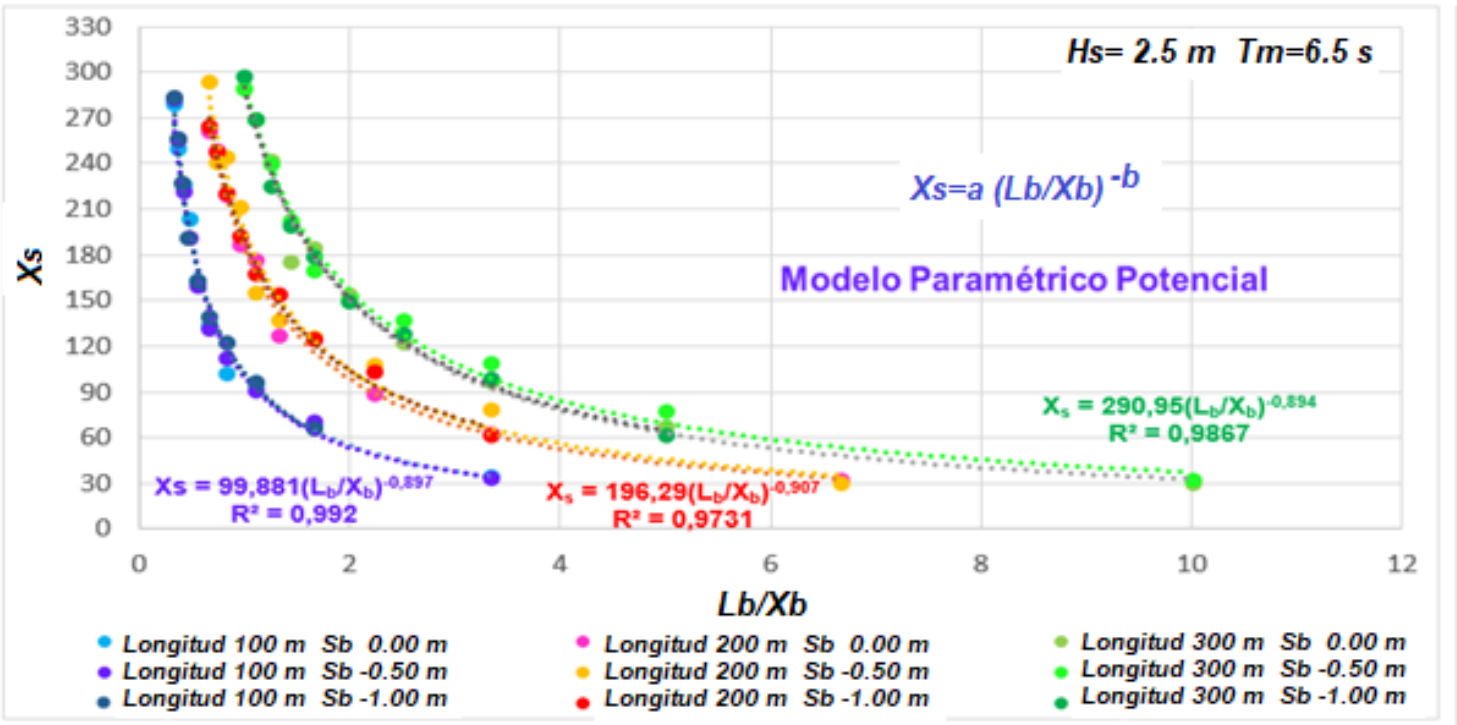

Figure 26. Relationship Length of breakwater / Initial distance to shore *vs*. distance to resulting shoreline (*Xs*). *Hs* = 2.5 m, *Tm* = 6.5 s. Source: Author's own.

The results obtained in the research allowed to establish predictive relationships on the behavior of the coastline (erosion/accretion) based on the dimensionless parameter (*Lb*/*Xb*), proposing a parametric model of a potential type that responds to the general formulation:

$$X_s = a\left(L_b/X_b\right)^{-b}$$

2022, Instituto Mexicano de Tecnología del Agua

Open Access bajo la licencia CC BY-NC-SA 4.0
(https://creativecommons.org/licenses/by-nc-sa/4.0/)

The parameter *a* and the exponent *b* are listed in Table 11, Table 12, and Table 13.

Table 11. Parameter *a* and exponent *b* of the potential function for breakwaters of length *Lb* = 100 m. Source: Author's own.

Hydrodynamics	Submergence (m)	*a*	*b*
Hs = 0.5 m *Tm* = 5.5 s	0.00	100	-1
	-0.50	99.50	-0.924
	-1.00	98.91	-0.978
Hs = 1.5 m *Tm* = 5.5 s	0.00	98.98	-0.970
	-0.50	103.05	-0.867
	-1.00	97.75	-0.956
Hs = 2.5 m *Tm* = 6.5 s	0.00	100.87	-0.888
	-0.50	99.88	-0.897
	-1.00	102.11	-0.893

Table 12. Parameter *a* and exponent *b* of the potential function for breakwaters of length *Lb* = 200 m. Source: Author's own.

Hydrodynamics	Submergence (m)	*a*	*b*
Hs = 0.5 m	0.00	200	-1

2022, Instituto Mexicano de Tecnología del Agua

Open Access bajo la licencia CC BY-NC-SA 4.0
(https://creativecommons.org/licenses/by-nc-sa/4.0/)

Tm = 5.5 s	-0.50	194.95	-0.938
	-1.00	196.51	-0.978
Hs = 1.5 m Tm = 5.5 s	0.00	189.68	-0.928
	-0.50	192.97	-0.893
	-1.00	196.40	-0.939
Hs = 2.5 m Tm = 6.5 s	0.00	184.26	-0.902
	-0.50	196.29	-0.973
	-1.00	189.60	-0.865

Table 13. Parameter *a* and exponent *b* of the potential function for breakwaters of length Lb = 300 m. Source: Author's own.

Hydrodynamics	**Submergence (m)**	**a**	**b**
Hs = 0.5 m Tm = 5.5 s	0.00	300	-1,00
	-0.50	290.95	-0.946
	-1.00	291.63	-0.965
Hs = 1.5 m Tm = 5.5 s	0.00	285.06	-0.971
	-0.50	283.60	-0.893
	-1.00	290.52	-0.945
Hs = 2.5 m Tm = 6.5 s	0.00	290.18	-0.948
	-0.50	290.95	-0.986

2022, Instituto Mexicano de Tecnología del Agua

Open Access bajo la licencia CC BY-NC-SA 4.0
(https://creativecommons.org/licenses/by-nc-sa/4.0/)

	-1.00	289.76	-0.932

As a practical result for the use of predictive relationships, a methodology consisting of four steps was developed, using the graphs in Figures 24, Figure 25, or Figure 26.

1. Calculate the *Lb*/*Xb* ratio

2. Plot the relationship *Lb*/*Xb* (abscissa axis) in the graph of Figure 24, Figure 25, or Figure 26 as appropriate with the swell and submergence defined as starting data.

3. Obtain, by the intercept of the abscissa axis with the curve corresponding to the breakwater length, the value *Xs* (distance between the formed coastline and the breakwater) on the ordinate axis.

4. Determine the expected response of the coast by subtracting from the initial distance to the coast *Xb* established in the design, the value *Xs* obtained from the graph. Answer (erosion or accretion) = *Xb* – *Xs*.

The application of the methodology is presented in the case study of the Meliá Varadero hotel. This hotel is located on a rocky massif, on both sides of which there are low terrace areas with lengths of 200 m and altitudes between 1.6 m and 2.5 m that make access to the beach difficult and limit its use as a bathing area (Figure 27).

2022, Instituto Mexicano de Tecnología del Agua

Open Access bajo la licencia CC BY-NC-SA 4.0
(https://creativecommons.org/licenses/by-nc-sa/4.0/)

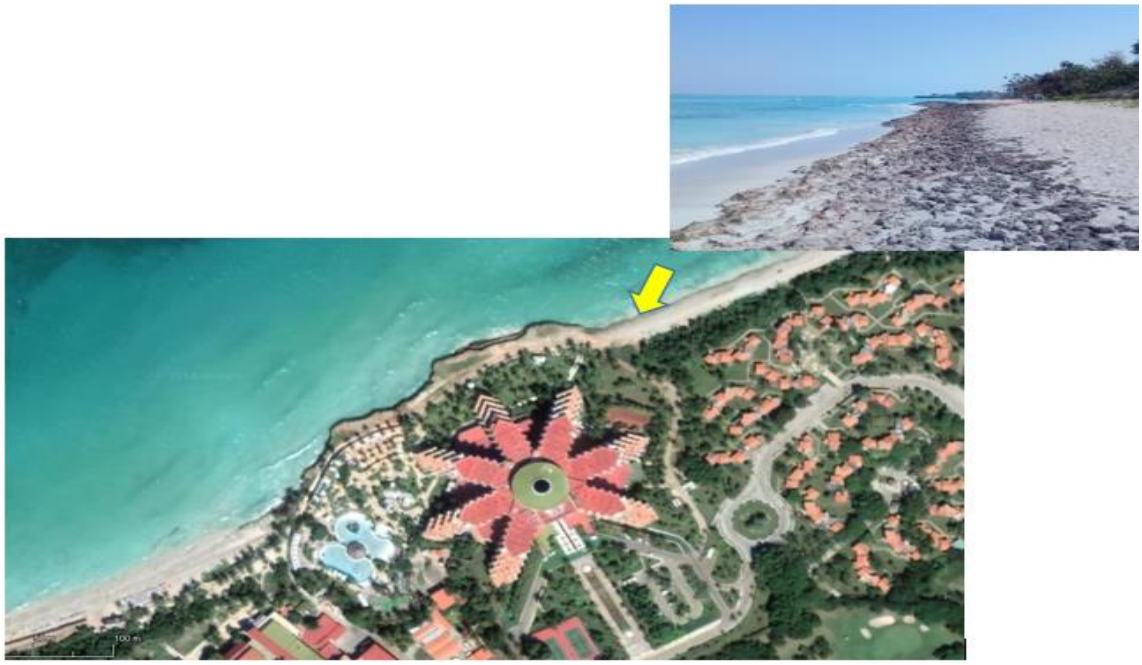

Figure 27. Location of the Meliá Varadero hotel. Source: Author's own.

The location of 100 m long submerged breakwaters is a viable solution to stabilize the beach. It is proposed to place it separated from the coast at a distance of 150 m with submergence of -0.50 m and a crest width of 10 m. The values of significant wave height Hs = 1.5 m and mean wave period *Tm* = 5.5 s are established.

1. Calculate the relationship *Lb*/*Xb* = 100 m / 150 m = 0.666.

2. The relation *Lb*/*Xb* = 0,666 is plotted in the graph of Figure 25, and the intercept with the 100 m length curve is obtained.

3. Value of the intercept on the ordinate axis *Xs* = 138 m.

4. Since the initial distance to the coast *Xb* is proposed to be 150 m, with this location the expected response of the shoreline is determined:

2022, Instituto Mexicano de Tecnología del Agua

Open Access bajo la licencia CC BY-NC-SA 4.0
(https://creativecommons.org/licenses/by-nc-sa/4.0/)

Answer = 150 m -138 m = 12 m.

The coastline will undergo a cumulative process with the formation of a 12 m wide overhang, as seen in Figure 28.

Figure 28. Formation on the beach of a 12 m wide spit due to the location of a 100 m long submerged breakwater. Source: Author's own.

Conclusions

2022, Instituto Mexicano de Tecnología del Agua

Open Access bajo la licencia CC BY-NC-SA 4.0
(https://creativecommons.org/licenses/by-nc-sa/4.0/)

The behavior of the currents and, therefore, the way the bottom changes is similar for breakwaters with different lengths. The zone of influence increases with the increasing length of the breakwater.

As the crest width increases, the transmission coefficient decreases, and the water levels in the sheltered area of the breakwater decrease, being more effective in dissipating the wave height.

The location of the breakwaters for the coast has a strong relationship with the morphological response of the beach, highlighting erosive or cumulative patterns.

Submergence is a parameter closely related to the transmission coefficient and the morphology of the beach. By increasing the submergence to levels of -1.00 m, the dissipative effect of the breakwater decreases, so the use of submersions with values greater than -1.00 m is not recommended.

Wave obliquity does not have a significant influence on the mode of the response of the coast or wave transmission, obtaining results that are very similar to those achieved with waves perpendicular to the coast.

It is determined that the functional design parameters of the submerged breakwaters that most influence the response of the beach are the distance to the coast, the length of the breakwater, and the submergence.

Predictive relationships are presented in the form of graphs, which respond to a parametric model of a potential type, where the evolution that the coastline will have according to dimensionless parameters can be known, a methodology being developed as a practical result for the functional design of the submerged breakwaters.

2022, Instituto Mexicano de Tecnología del Agua

Open Access bajo la licencia CC BY-NC-SA 4.0
(https://creativecommons.org/licenses/by-nc-sa/4.0/)

Acknowledgments

The authors wish to thank all those people who have allowed, helped, and collaborated with the obtaining of the results referred to in this work.

References

Córdova, L., Hernández, K., & Benítez, H. (2017). Modelación matemática de procesos morfológicos en playas con rompeolas sumergidos. *Ingeniería Hidráulica y Ambiental*, 38(1), 59-71.

Calabrese, M., Vicinanza, D., & Buccino, M. (2008). 2D Wave setup behind submerged breakwaters. *Ocean Engineering Journal*, 35, 1015-1028.

García, C. (2005). *Actuaciones para el control de la erosión en playas biogénicas. El caso de la playa de Varadero* (tesis presentada en opción al grado científico de Doctor en Ciencias Geográficas), Instituto de Geografía Tropical, La Habana, Cuba.

Hernández, K., & Córdova, L. (2015). Simulación matemática de la interacción oleaje-estructuras de protección costera. *Ingeniería Hidráulica y Ambiental*, 36(3), 74-87.

Hernández, K., & Córdova, L. (2016). Calibración y validación de un modelo matemático para la simulación de los cambios morfológicos durante eventos extremos en una playa del Caribe. *Tecnología y ciencias del agua*, 7(3), 135-153. DOI: 10.24850/j-tyca-imta

2022, Instituto Mexicano de Tecnología del Agua

Open Access bajo la licencia CC BY-NC-SA 4.0
(https://creativecommons.org/licenses/by-nc-sa/4.0/)

Makris, V., & Memos, C. (2007). Wave transmission over submerged breakwaters: performance of formulae and models. *Proceedings of the Sixteenth International Offshore and Polar Engineering Conference*, Lisbon, Portugal.

Papadopoulos, D. (2012). *Scour below the toe of breakwaters* (thesis submitted for the degree of Master of Science in Hydraulic Engineering), Delf University of Technology, The Netherlands.

Ranasinghe, R., Larson, M., & Savioli, J. (2010). Shoreline response to a single shore- parallel submerged breakwater. *Coastal Engineering*, (57),1006-1017. DOI: 10.1016/j.coastaleng.2010.06.002

Roelvink, D., Reniers, A., van Dongeren, A., van Thiel-de-Vries, J., McCall, R., & Lescinski, J. (2009). Modelling storm impacts on beaches, dunes and barrier islands. *Coastal Engineering*, 56, 1133-1152. DOI: 10.1016/j.costaleng.2009.08.006

Vanlishout, V. (2008). *Oblique wave transmission through rough impermeable rubble mound submerged breakwaters* (thesis of the Master of Science degree in Civil Engineering), Ghent University, The Netherlands.